CHAPTER IV
RESULTS AND DISCUSSION

4.1 BET Surface Area, Particle Density, Structural Density and Pore Volume of the Adsorbents

The different adsorbents (mesoporous and macroporous alumina denoted as m-Al_2O_3 and M-Al_2O_3, respectively) were characterized by using nitrogen adsorption/desorption at 77 K and mercury porosimetry methods, to study the properties of the porous materials in terms of surface area, porosity and porous structure. The properties of both porous aluminas are listed in Table 4.1 and 4.2.

Table 4.1 Properties of adsorbents characterized by nitrogen adsorption/desorption method at 77 K

Adsorbents (IFP Reference)	Properties				
	S_{BET} (m^2/g)	V_μ [a] (t-plot) (cm^3/g)	V_m [b] (B.J.H.-desorption) (cm^3/g)	$V_m + V_\mu$ (P/P_0=0.99) (cm^3/g)	V_m (cm^3/g)
m-Al_2O_3 (94843)	278	0.000	0.797	0.752	0.752
M-Al_2O_3 (94844)	194	0.000	0.552	0.523	0.523

[a] V_μ is a microporous volume.

[b] V_m is a mesoporous volume.

Table 4.2 Properties of adsorbents by using the Mercury porosimetry

Adsorbents (IFP Reference)	Properties				
	Particle Density (g/cm^3)	Structural Density (g/cm^3)	V_m (cm^3/g)	V_M [a] (cm^3/g)	$V_m + V_M$ (cm^3/g)
m-Al_2O_3 (94843)	0.914	2.806	0.643	0.009	0.652
M-Al_2O_3 (94844)	1.008	2.994	0.481	0.151	0.632

[a] V_M is a mesoporous volume.

According to Table 4.1, m-Al_2O_3 has higher in B.E.T. surface area than M-Al_2O_3. It is observed that the B.E.T. surface area of m-Al_2O_3 is 278 m^2/g and the B.E.T. surface area of M-Al_2O_3 is 194 m^2/g. For the porous volume, it was determined that there are no micropores for alumina based adsorbents. In the same basis of one gram of adsorbent, m-Al_2O_3 has higher in mesoporous volume than M-Al_2O_3. The higher in mesoporous volume constitutes to higher in B.E.T. surface area.

Similar results were found by Atireklapwarodom (2009) for the alumina. Furthermore, she studied on the incipient wetness impregnation method by varying the metal loading. It was found that since the metal, Cu^{2+}, covers the surface of the adsorbent, the surface area is decreased. It was concluded that the greater is the metal loading, the lower is the mesoporous volume which corresponds to the decrease of surface area.

From Table 4.2, M-Al_2O_3 has a higher particle density than m-Al_2O_3. For the mesoporous volume determined with mercury intrusion, it shows similar result compare to nitrogen adsorption/desorption results: m-Al_2O_3 has higher mesoporous volume than M-Al_2O_3. For macroporous volume, m-Al_2O_3 has a small amount compare to those of M-Al_2O_3.

4.2 Temperature-Programmed Reduction (TPR) Characterization

From the literature, Cu^+ is known for its π-complexation ability. It can increase the capacity and selectivity of the adsorption of organic sulfur compounds.

In this study, incipient wetness impregnation method was used to manipulate the adsorbent. It requires metal solution as a media to impregnate metals on the adsorbent. To impregnate Cu^+ on the adsorbent, CuCl was chosen. Unfortunately, CuCl is inappropriate because it is water-insoluble (as water was preferably to be used as a solvent). Thus $CuCl_2$ was used instead due to it is high solubility in water. For this reason, it is necessary to reduce Cu^{2+} to Cu^+ by means of hydrogen. To study the reduction condition, TPR experiments were carried out to study the reduction step and reduction temperature.

$CuCl_2$ impregnated on m-Al_2O_3 (0.1 g approximately) was held in place by glass wool plugs. The gas mixture used was 4.95% H_2 in N_2 at flow rate of 20

cm^3/min, the heating rate was 10 °C/min. It was first heated up to 900 °C, hold at this temperature for 2 hours, and after that it was cooled down to ambient temperature. The intensity measured by thermal conductivity detector (TCD) indicates H_2 consumption.

The result of TPR experiment corresponding to 30% Cu/m-Al_2O_3 is shown in Figure 4.1.

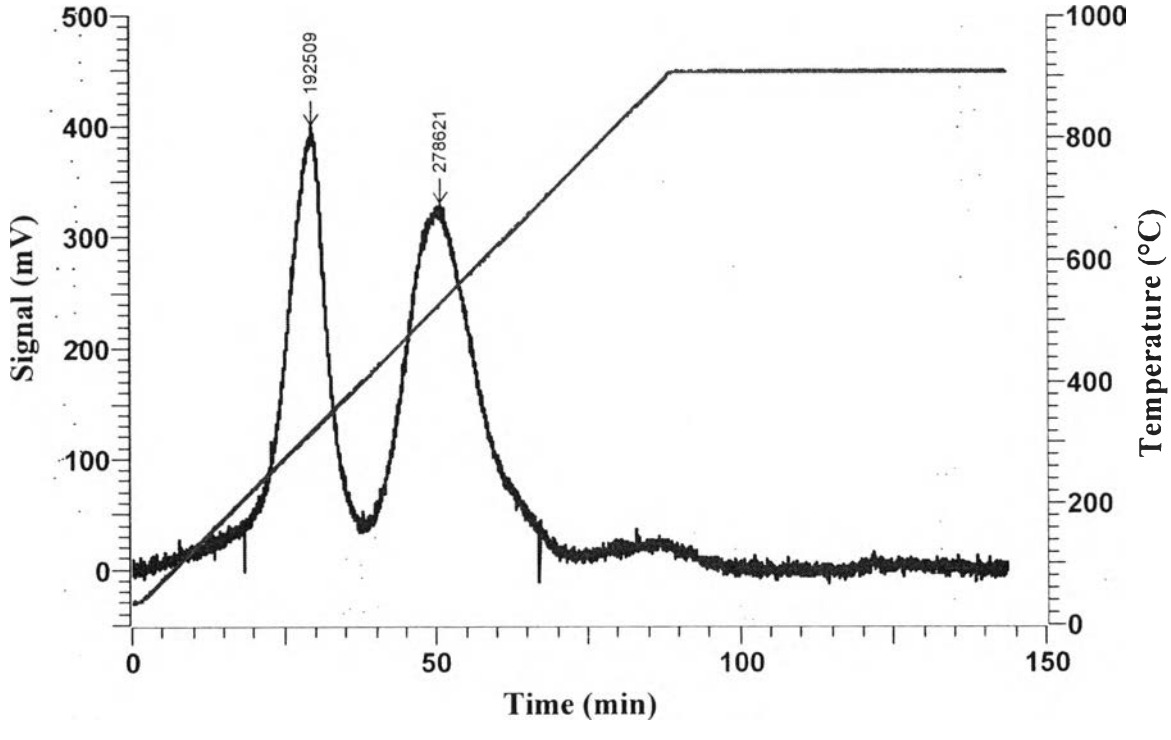

Figure 4.1 Temperature-programmed reduction (TPR) of 30% Cu/m-Al_2O_3 in 4.95% H_2 in N_2 at 900 °C.

Figure 4.1 shows the result from TPR experiment of 30% Cu/m-Al_2O_3 in 4.95% H_2 in N_2 at 900 °C. Two main distinct peaks corresponding to two steps of reduction plus another small one were detected and the results were summarized in Table 4.3.

Table 4.3 At peak TPR results of 30% Cu/m-Al_2O_3

Peak Number	Temperature (°C)	Reduction		
		Start (°C)	Stop (°C)	Total time (min)
1	316	118	403	18.7
2	529	403	742	28.1
3	850	–	–	–

The temperature at the first peak (192509) is an appropriate temperature to reduce Cu^{2+} to Cu^{+} which is 316 °C. The above results indicate that almost 100% of Cu^{2+} has been reduced into Cu^{+} at around 400 °C for 20 minutes in presence of H_2. And the temperature at the second peak (278621) is an appropriate temperature to reduce Cu^{+} to Cu^{0} which is 529 °C. Cu^{+} has totally been reduced to Cu^{0} at around 740 °C for 30 minutes in presence of H_2. For the third peak, it was detected around 850 °C.

As mentioned above, the first peak indicated the reduction from Cu^{2+} to Cu^{+}, and the second peak indicated the reduction from Cu^{+} to Cu^{0}, but for third peak, detected around 850 °C, it is not an effect of the reduction. So it could be interesting to study the morphological modification of m-Al_2O_3 subjected to high temperature.

This TPR results are used to determine the condition of reduction step and its effect to $CuCl_2$ impregnated on both alumina. Those adsorbents were needed to be reduced to Cu^{+} only (not further reduced to Cu^{0}). If higher or inappropriate reduction temperature is applied, it will reduce Cu^{2+} to Cu^{+} and further reduce Cu^{+} to Cu^{0}. As Cu^{0} has no π-complexation activity hence it will lose the selectivity and reactivity of the adsorbent on adsorptive desulfurization.

4.3 Scanning Electron Microscopy (SEM)

The porosity within the adsorbents and the metal dispersion over the adsorbents were studied by using SEM coupled with Energy Dispersive X-ray Spectroscopy (EDX). It was performed on the cut impregnated samples. The samples were fractured at the cross section to study the internal surface. The cut samples were coated with Pt before examination. Simultaneaous detection of Cu or Ni was performed by Energy-dispersive X-ray spectroscopy (EDX) which was coupled with SEM. The analysis was done at both PPC and IFP Energies nouvelles. At PPC it was done at a resolution of 30 k, a working distance (WD) of 3.8 mm at 1.5 kV under high vacuum and ambient temperature and At IFP Energies nouvelles it was done at a resolution of 60 k, a working distance (WD) of 8.3 mm at 15.0 kV under high vacuum and ambient temperature. These samples were observed by backscattered electrons (chemical contrast) mode.

Figure 4.2 shows the SEM images of 30% Cu/m-Al_2O_3 by chemical contrast mode. Focusing on the Figure 4.2 (a), it shows that there is a deposition inside the adsorbent and there are agglomerates of $CuCl_2$ in some position on the surface of the adsorbent. It implies that the incipient wetness impregnation method is a promising method for metal impregnation, nevertheless, the dispersion of the $CuCl_2$ seems to be heterogeneous. It is observed that there is a big deposition of $CuCl_2$ on the surface as shown in Figure 4.2 (b). In Figure 4.2 (c), it shows the undefined shape of the $CuCl_2$ crust with an average thickness of 10 μm and up to 80 μm in some positions. The crust is composed of compacts of faceted particles, with size ranging from 100 nm to 1 μm.

Figure 4.3 shows the SEM images of 30% Cu/m-Al_2O_3 modified with CA with the molar ratio Cu/CA of 10 by chemical contrast mode. Corresponding to Figure 4.3 (a) and (b), it is also observed the form of $CuCl_2$ clusters, of undefined shape particles, which distribute throughout the adsorbent. From the observation, the size of these clusters is around 2 μm. Figure 4.3 (c) and (d) shows a "bug chestnut" type cluster at trefoils of macropore. Theses clusters size is 4 μm in diameter approximately.

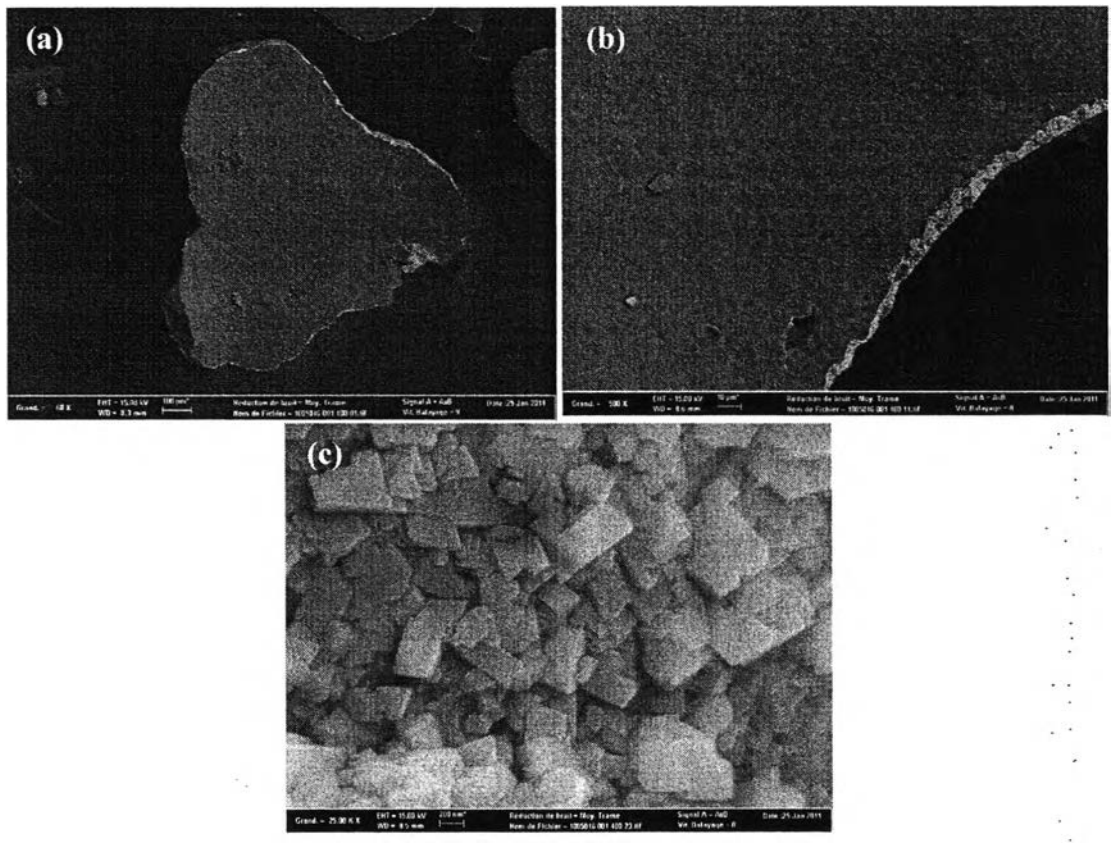

Figure 4.2 SEM images of 30% Cu/m-Al_2O_3: (a) cross section of 30% Cu/m-Al_2O_3, (b) cluster on the edge of 30% Cu/m-Al_2O_3, (c) form of clusters deposited on the surface of 30% Cu/m-Al_2O_3.

Comparing Figure 4.2 with Figure 4.3 in order to study the effect of dispersing agent shows that the metal ($CuCl_2$) dispersion of modified adsorbent by CA is better than those of unmodified adsorbent. As CA is claimed to be used to disperse the Cu^{2+} throughout the adsorbents for metal dispersion enhancement, SEM characterization results has confirmed this hypothesis. It is clearly shown that the dispersion of $CuCl_2$ is improved after modification with dispersing agent.

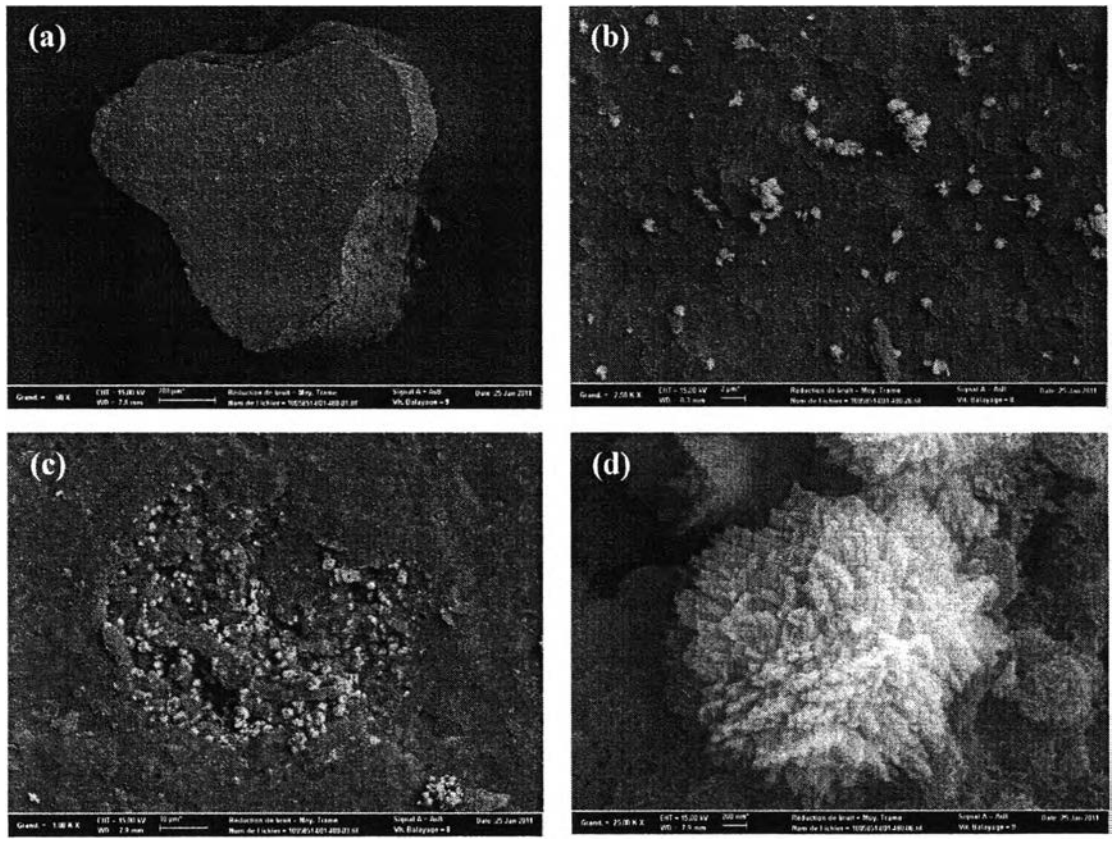

Figure 4.3 SEM images of 30% Cu/m-Al_2O_3 modified with CA with the molar ratio Cu/CA of 10: (a) cross section of 30% Cu/m-Al_2O_3 modified with CA with the molar ratio Cu/CA of 10, (b) metal on the surface, (c) and (d) a "bug chestnut" type cluster.

In order to establish the role of π-complexation adsorbents, it is necessary to reduce the Cu^{2+} to Cu^{+} by means of reduction. The H_2 reduction was used to reduce copper halides impregnated adsorbents with and without modification with CA in order to study the effect of heat treatment (reduction) on the metal dispersion.

The reduced 30% Cu/m-Al_2O_3 and reduced 30% Cu/m-Al_2O_3 modified with CA (Cu/CA = 10) were studied by SEM. The SEM images of reduced 30% Cu/m-Al_2O_3 and reduced 30% Cu/m-Al_2O_3 modified with CA (Cu/CA = 10) are shown in Figure 4.4 and Figure 4.5, respectively.

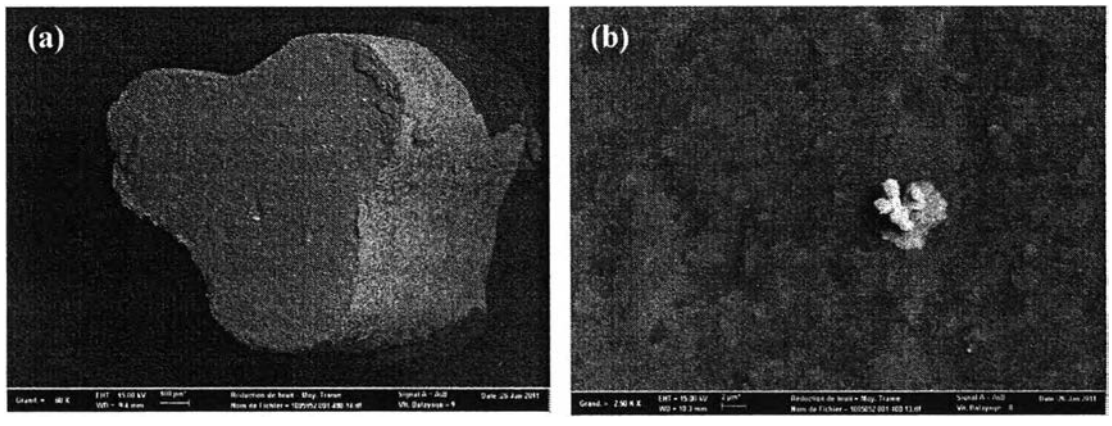

Figure 4.4 SEM images of reduced 30% Cu/m-Al_2O_3: (a) cross section of reduced 30% Cu/m-Al_2O_3, (b) clusters form.

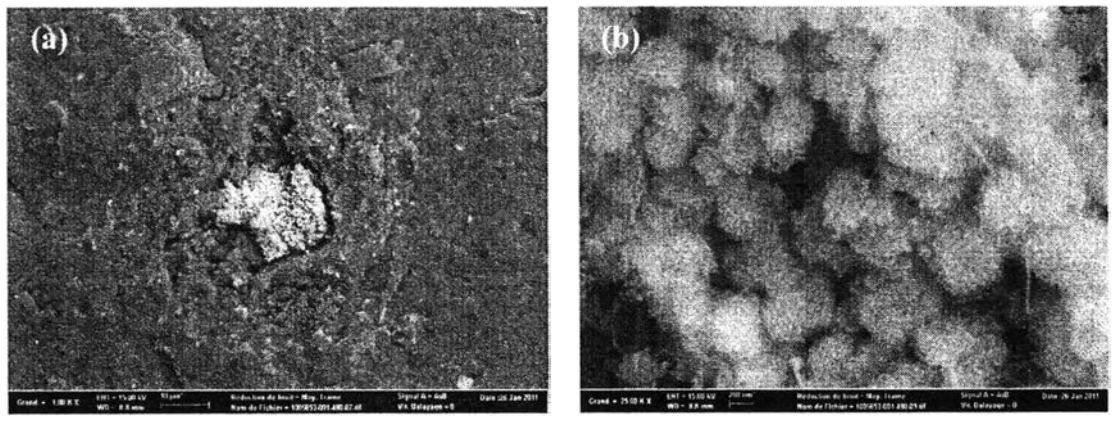

Figure 4.5 SEM images of reduced 30% Cu/m-Al_2O_3 modified with CA with the molar ratio Cu/CA of 10: (a) "bug chestnut" typed clusters, (b) a "bug chestnut" type cluster.

Figure 4.4 (a) shows the metal (CuCl) is dispersed throughout the adsorbents. The EDX analysis shows the presence of Cu and Cl whereas it is invisible in the images. It is also observed that there are rare clusters with poorly defined shape within the sample as shown in Figure 4.5 (b). The size of these clusters is approximately 5 μm.

In case of reduced 30% Cu/m-Al_2O_3 modified with CA, the EDX analysis also shows the presence of Cu and Cl (but it is invisible in the images) and it shows that the metal (CuCl) dispersion is also enhanced throughout the adsorbents. Figure 4.5 (a) shows a "bug chestnut" type cluster located at the trefoils of macropore. It is in agreement with 30% Cu/m-Al_2O_3 modified with CA results, showing also a "bug chestnut" type cluster. Due to this type of clusters are only found in the adsorbent modified with CA, thus, this form of clusters may correspond to the CA decomposition after heat treatment. Figure 4.5 (b) shows the appearance of these clusters with a size of 1 μm approximately.

After performing the reduction, it is shown that the metal dispersion is better on both with and without dispersing agent modification. It is clearly shown that the clusters are reduced in terms of their size and quantity, therefore, the reduction step enhances the metal dispersion.

4.4 X-Ray Diffraction (XRD)

X-ray diffraction (XRD) was performed to analyze the chemical species on the adsorbents. To study the phase change of $CuCl_2$, 30% Cu/m-Al_2O_3 and 30% Cu/m-Al_2O_3 modified with CA were analyzed. The diffractograms are shown in Figure 4.6. The pure $CuCl_2$ (reference) was also analyzed. Their chromatograms are shown in Figure 4.7.

Figure 4.6 shows the diffractograms of 30% Cu/m-Al_2O_3 and 30% Cu/m-Al_2O_3 modified with CA. It is observed that the diffractograms of both adsorbents are perfectly superimposed. Comparing the diffractograms of both adsorbents with the diffractograms of m-Al_2O_3 (reference) demonstrates the unique peaks which are only detected for impregnated adsorbents. The copper chloride hydroxide—$CuCl_2.3Cu(OH)_2$—is detected whereas $CuCl_2$ is not detected which is unexpected to occur. It indicates that the $CuCl_2$ reacts after making an impregnation, therefore, the stability of $CuCl_2$ when exposed to the air and water is interesting to study in order to confirm the behavior of this chemical.

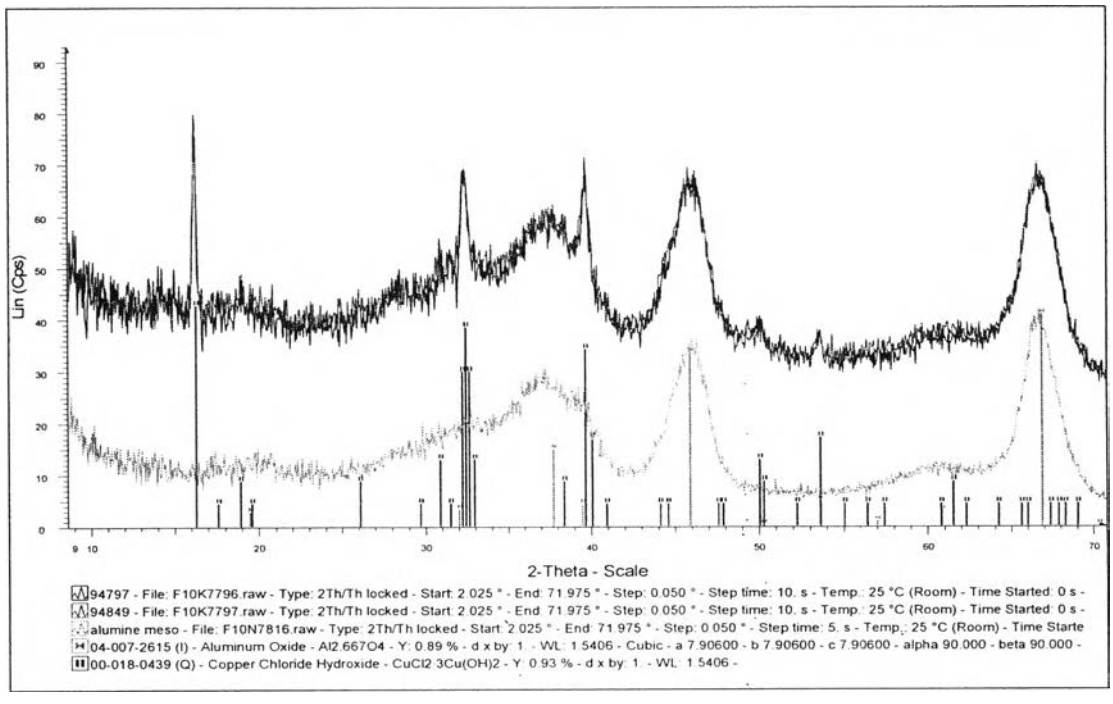

Figure 4.6 Chromatograms of 30% Cu/m-Al_2O_3 and 30% Cu/m-Al_2O_3 modified with CA adsorbents.

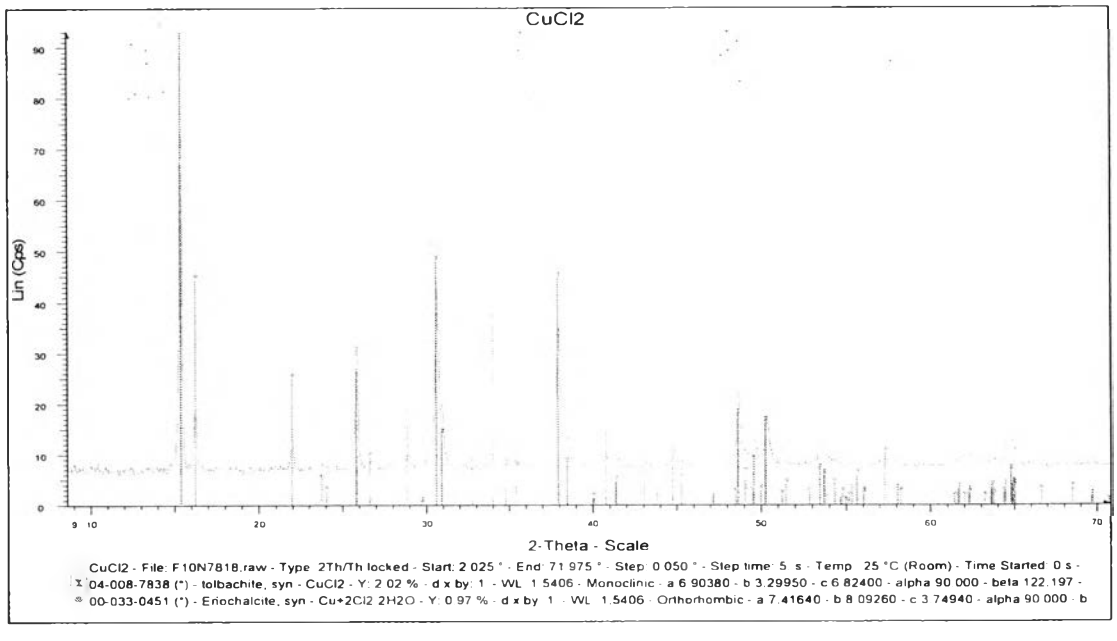

Figure 4.7 Diffractograms of $CuCl_2$.

Figure 4.7 shows the diffractograms of $CuCl_2$ (reference). The phases of $CuCl_2$ and eriochalcite ($CuCl_2.2H_2O$) are identified. It is observed that the $CuCl_2$ is unstable. It has become swollen and turned from original color, which is brown, to green which is unstable when it expose to the atmosphere.

In order to study the phase change of CuCl, reduced 30% Cu/m-Al_2O_3 and reduced 30% Cu/m-Al_2O_3 modified with CA were characterized. Phase change of pure CuCl (as a reference) is also studied. Their diffractograms are shown in Figure 4.8 and 4.9, respectively.

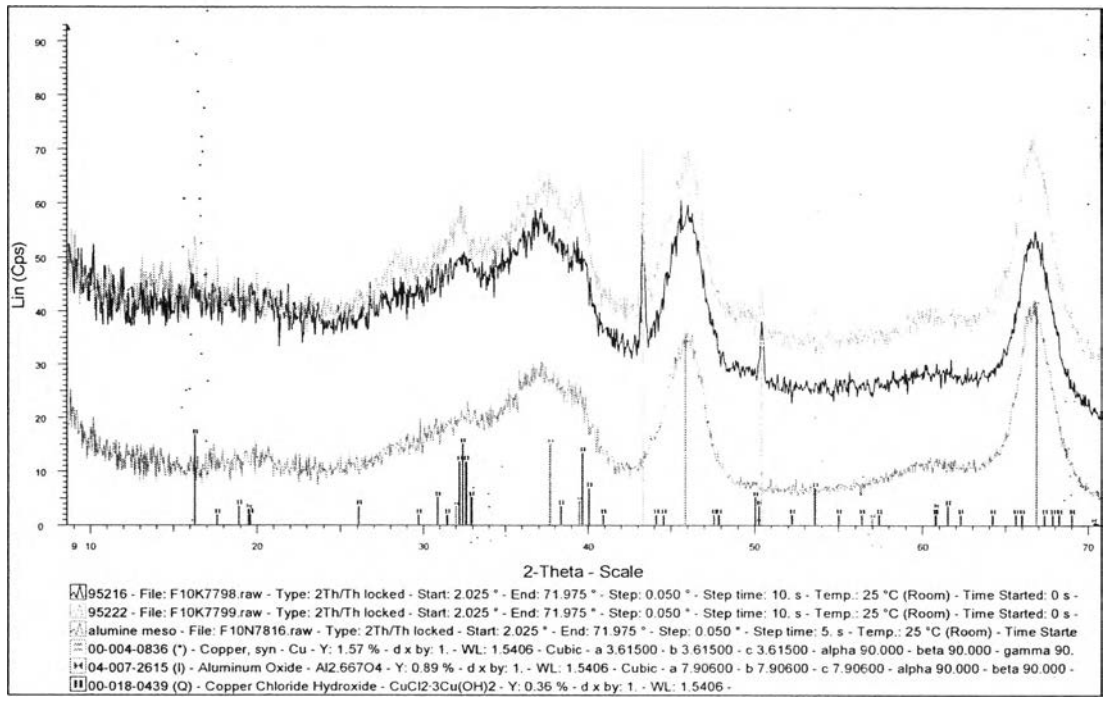

Figure 4.8 Diffractograms of reduced 30% Cu/m-Al_2O_3 and reduced 30% Cu/m-Al_2O_3 modified with CA.

Figure 4.8 shows the diffractograms of reduced 30% Cu/m-Al_2O_3 and reduced 30% Cu/m-Al_2O_3 modified with CA. It is observed that the diffractograms of both adsorbents are superimposed. Comparing the diffractograms of both adsorbents with the diffractograms of m-Al_2O_3 (reference) demonstrates the unique peaks which are only detected for reduced impregnated adsorbents. A little copper

chloride hydroxide—$CuCl_2.3Cu(OH)_2$—and copper (Cu) are detected whereas CuCl is not detected.

Before making a reduction step, impregnation of $CuCl_2$ was achieved, then was reduced from Cu^{2+} ($CuCl_2$) to Cu^+ (CuCl) at an appropriate condition. As shown in the previous part, the $CuCl_2$ is unstable and changes its form after impregnation ($CuCl_2$ was not detected). Thus, CuCl cannot be detected due to the original $CuCl_2$ before reduction has changed its form.

The remaining copper chloride hydroxide and copper implies that the reduction condition was inappropriate. In case of copper chloride hydroxide, it indicates that the reduction of Cu^{2+} to Cu^+ is incomplete. For the case of copper, it indicates that the adsorbents were too much reduced. Therefore, the modification of heat treatment is recommended to study.

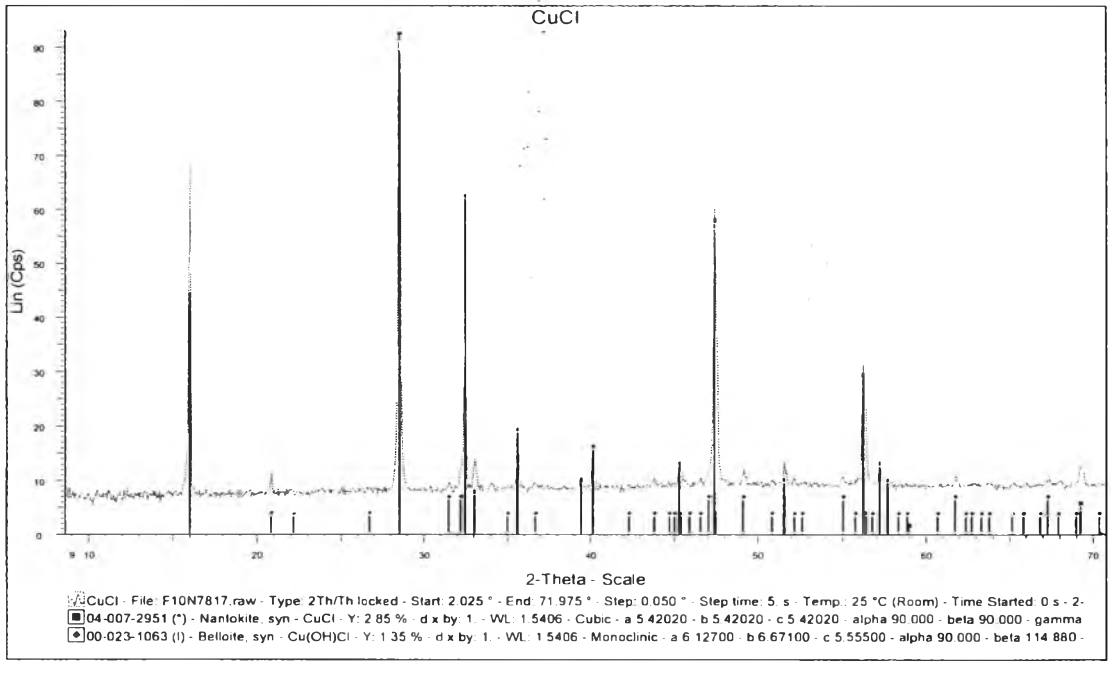

Figure 4.9 Diffractograms of CuCl.

Figure 4.9 shows the diffractograms of CuCl (reference). CuCl and belloite (Cu(OH)Cl) phases can be detected. It means that the CuCl phase is unstable.

4.5 X-Ray Photoelectron Spetroscopy (XPS)

This technique was used to study the chemical composition on the solid surface. XPS is carried out to analyze the chemical composition about 5–10 nm below the surface of the samples.

In this analysis, copper chloride activated on alumina with and without dispersing agent modification, and, with and without H_2 treatment were studied. CuCl and $CuCl_2$ were used as reference chemicals.

In case of reference chemicals, samples were prepared in a glove box in order to protect them from air for humidity and O_2 control. Indeed, under ambient atmosphere, samples changed their color and morphology. Obviously, they were oxidized or hydroxylated.

The reference chemical results and the analysis results (wt%) are shown in Table 4.4 and Table 4.5, respectively.

Table 4.4 XPS analysis results (reference chemicals) (wt%)

Elements Detected	Reference Chemicals	
	CuCl	$CuCl_2$
Cu	57.00	46.10
Cl	27.70	45.40
O	5.30	2.90
Cl/Cu (mol%)	0.87	1.77

From the Table 4.4, it shows that the Cl/Cu ratio of CuCl and $CuCl_2$ are 0.87 and 1.77, respectively, which are not equal to 1 and 2, respectively, as it should be. There is another elements detected which is oxygen. It implies that the CuCl and $CuCl_2$ have been transformed into another morphology or change their chemical according to oxygen detected. It is in agreement with the XRD results which are mentioned before that the CuCl and $CuCl_2$ are instable when exposing to the air, they are oxidized.

Table 4.5 XPS analysis results (wt%)

Elements Detected	Samples			
	mCu3024[a]	mCA10Cu3024[b]	mCu3024H2[c]	mCA10Cu3024H2[d]
Cu	2.45	2.95	4.00	4.10
Cl	1.75	2.10	1.90	1.50
Al	50.40	50.05	49.60	50.65
O	39.10	39.10	39.40	39.05
Cl/Cu (mol%)	1.27	1.26	0.85	0.67

[a] 30% Cu/m-Al_2O_3.

[b] 30% Cu/m-Al_2O_3 modified with CA (Cu/CA ratio of 10).

[c] reduced 30% Cu/m-Al_2O_3.

[d] reduced 30% Cu/m-Al_2O_3 modified with CA (Cu/CA ratio of 10).

Table 4.5 shows the XPS analysis results of 30% Cu/m-Al_2O_3 with and without dispersing agent modification, and, with and without H_2 treatment, respectively. Cu, Cl, Al and O elements are detected which correspond to CuCl, $CuCl_2$ and alumina (Al_2O_3). Applying this technique to the metal dispersion study, the amount of Cu detected is concerned. If there is a good dispersion, the Cu must be easily detected, thus, amount of Cu detected is higher. The amount of Cu detected based on the same amount of metal loading (30% of theoretical monolayer coverage) for 30% Cu/m-Al_2O_3 is 2.45 wt%, for 30% Cu/m-Al_2O_3 modified with CA (Cu/CA ratio of 10) is 2.95 wt%, for reduced 30% Cu/m-Al_2O_3 is 4.00 wt% and for reduced 30% Cu/m-Al_2O_3 modified with CA (Cu/CA ratio of 10) is 4.10 wt%. The non modified and modified adsorbents with dispersing agent are compared. It seems that the amount of Cu detected is quite similar which are 2.45 compare to 2.95 wt% of Cu detected and 4.00 compare to 4.10 wt% of Cu detected. There is a distinction on two samples having undergone in H_2 treatment which there is a better quantification of Cu. Therefore the effect of dispersing agent modification on metal dispersion is limited. The main effect on metal dispersion is H_2 treatment. It is noted that the XPS analysis is an analysis of extreme surface, then this could be interpreted as a better dispersion of CuCl on the surface of alumina after having undergone in H_2 treatment.

4.6 Temperature-Programmed Desorption (TPD) Experiments by Using Thermogravimetric Analysis Coupled with Mass Spectrometer (TGA-MS)

This technique was used to determine the adsorption or desorption of sulfur compounds on the adsorbents. The experiments were performed by thermogravimetric analysis coupled with mass spectrometer (TGA-MS). In this study, simulated hydrocarbon feeds (the solution of dibenzothiophene (DBT) in toluene with different concentrations of 1, 3 and 5 wt% DBT), pure toluene and pure thiophene solutions were used. Non-impregnated aluminas (both m-Al_2O_3 and M-Al_2O_3), impregnated aluminas (copper impregnated on both aluminas), impregnated aluminas modifed with dispersing agent (citric acid, CA) and reduced aluminas were used as adsorbents. The results were obtained to study the behavior of DBT, thiophene and toluene adsorption on the adsorbents; to study the effect of aromatics on the selective desulfurization by adsorption; to study the effect of dispering agent on the metal dispersion; to study the specific adsorption on π-complexation adsorbents and the effect of size of sulfur compounds was also studied.

4.6.1 Desorption Behavior

The desorption profiles of pure toluene, solution of DBT in toluene, and pure thiophene solution adsorbed on m-Al_2O_3 and M-Al_2O_3 are illustrated in Figure 4.10 and Figure 4.11, respectively, and the desorption profiles of 1, 3 and 5 wt% DBT in toluene adsorbed on m-Al_2O_3 and M-Al_2O_3 are illustrated in Figure 4.12 and Figure 4.13, respectively.

Figure 4.10 and Figure 4.11 show the desorption profiles of pure toluene, 3 wt% DBT in toluene and pure thiophene solutions adsorbed on m-Al_2O_3 and M-Al_2O_3, respectively. The peaks of this curve correspond to the desorption temperature. The different nature of adsorption will lead to different desorption behavior.

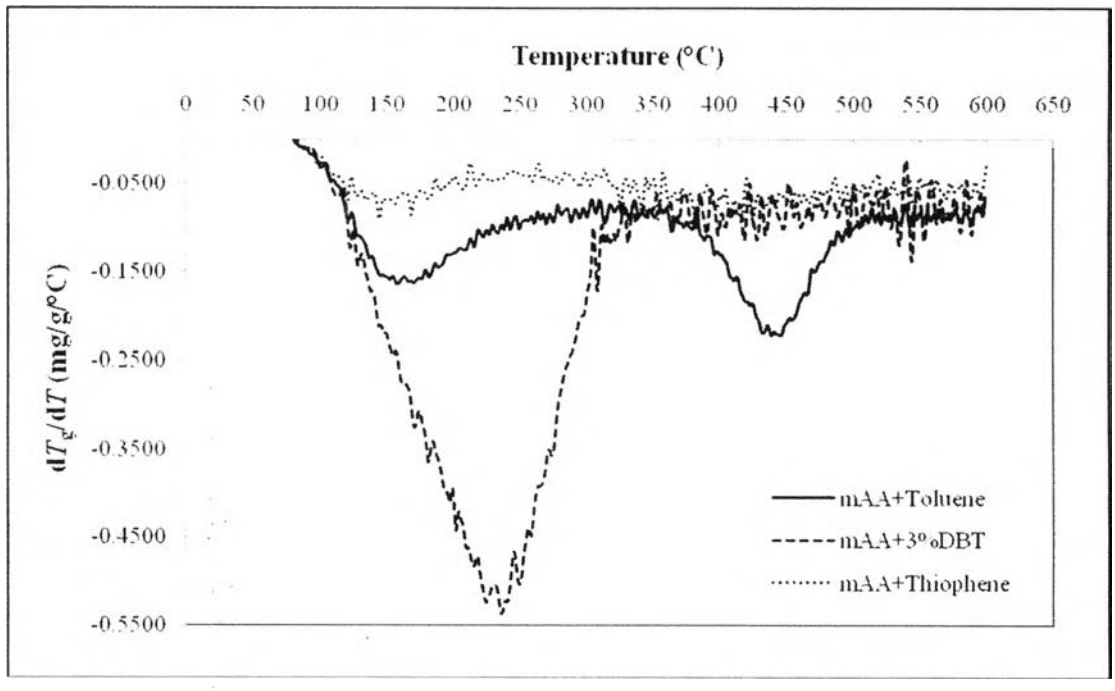

Figure 4.10 Desorption profiles of pure toluene, 3 wt% DBT in toluene and pure thiophene solutions adsorbed on m-Al_2O_3.

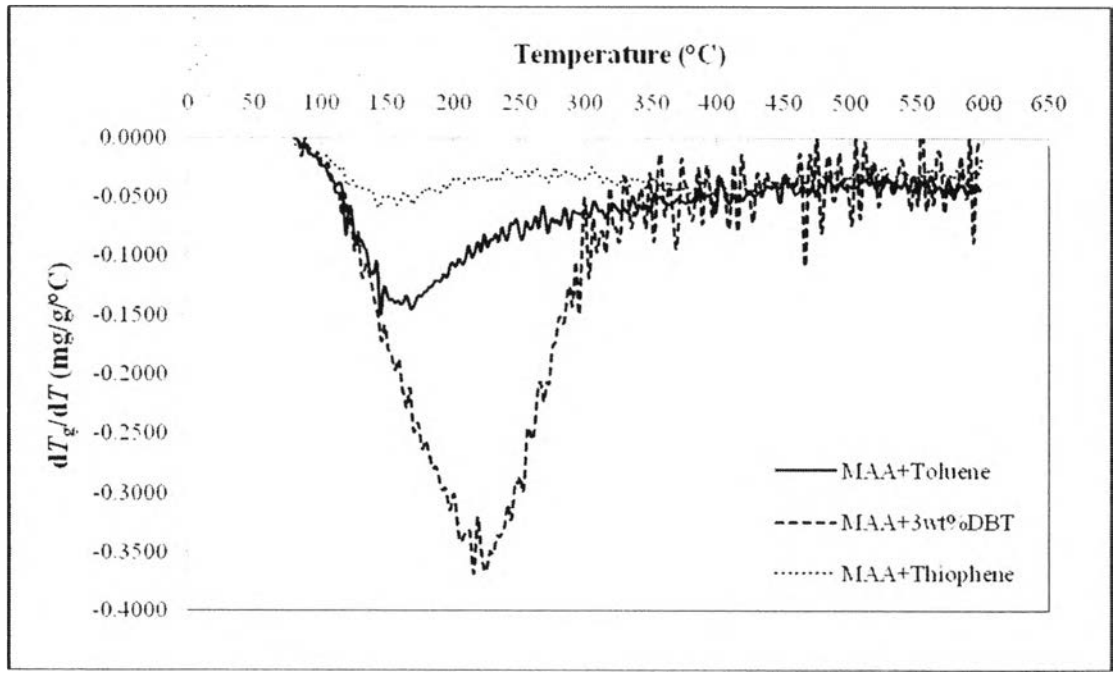

Figure 4.11 Desorption profiles of pure toluene, 3 wt% DBT in toluene and pure thiophene solutions adsorbed on M-Al_2O_3.

The desorption temperature of toluene is approximately 150 °C, the desorption temperature of thiophene is approximately 160 °C and the desorption temperature of DBT is approximately 240 °C for both aluminas, which is the highest desorption temperature among the solutions studied. DBT is the biggest molecule (molecular weight is 184.26 g/mol) compared to toluene and thiophene. It is stronger adsorbed and, thus, it is harder to desorb which leads to a higher desorption temperature. The higher desorption temperarture corresponds to the higher adsorbate–adsorbent interactions. Therefore, the adsorbate–adsorbent interaction of DBT is stronger than those of thiophene and toluene, respectively.

In Figure 4.10, there is another peak at high temperature around 450 °C. It may correspond to the modification of the solid surface (dehydroxylation of alumina).

Figure 4.12 shows the desorption profiles of 0, 1, 3 and 5 wt% DBT in toluene adsorbed on m-Al_2O_3. The desorption temperature of toluene is approximately 150 °C. The desorption temperature of 1, 3 and 5 wt% DBT in toluene are approximately 250, 240 and 230 °C, respectively. For the solution of DBT in toluene, there is only extinct peak which correspond to the desorption of DBT alone. The higher amount of DBT leads to lower desorption temperature. If there is only monolayer adsorption, the desorption temperature should be the same. It implies that there is a multilayer adsorption due to the peak shifts to lower desorption temperature when the amount of DBT increases.

At low coverage, the active sites are occupied by the adsorbate. At high coverage, these mesopores would be expected to filled with adsorbate and once they are filled, further adsorption can only occur through multilayer formation on the surface of the solid. The adsorption energy of multilayer adsorption is lower than those on monolayer adsorption which leads to lower desorption temperature. The area under the curve correspond to the amount of adsorbate which is adsorbed on the adsorbent. Thus, the area under the curve of 5 wt% DBT in toluene adsorbed on m-Al_2O_3 is more than those of 3 and 1 wt% DBT in toluene adsorbed on m-Al_2O_3 respectively.

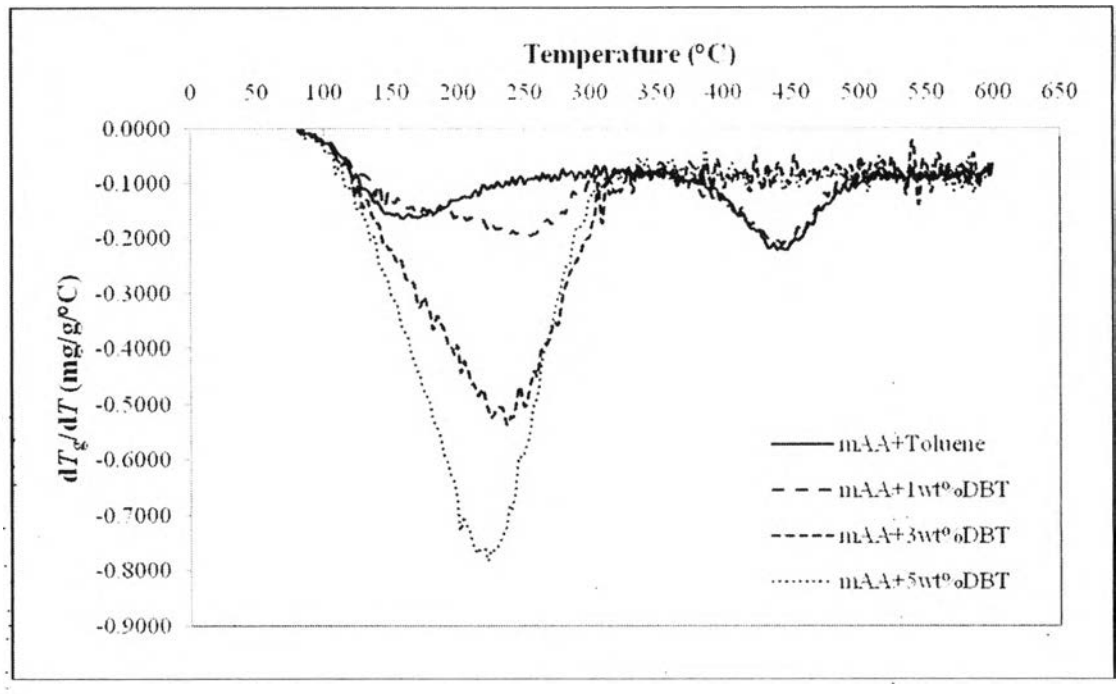

Figure 4.12 Desorption profiles of 0, 1, 3 and 5 wt% DBT in toluene adsorbed on m-Al_2O_3.

4.6.2 The Effect of Type of the Adsorbents

As shown in Figure 4.10 and Figure 4.11, there are no many differences of the desorption temperature of those solutions adsorbed on both mesoporous and macroporous alumina. It is concluded that the effect of type of the adsorbents is insignificant.

4.6.3 The Effect of Dispersing Agent on the Metal Dispersion

To study the effect of dispersing agent that used to enhance the metal dispersion, the different desorption profiles of thiophene adsorbed on different adsorbents were studied.

Figure 4.13 and Figure 4.14 show the desorption profiles of thiophene adsorbed on m-Al_2O_3, reduced 30% Cu/m-Al_2O_3 and reduced 30% Cu/m-Al_2O_3 modified with CA (Cu/CA=10); and, M-Al_2O_3, reduced 30% Cu/M-Al_2O_3 and reduced 30% Cu/M-Al_2O_3 modified with CA (Cu/CA=10), respectively.

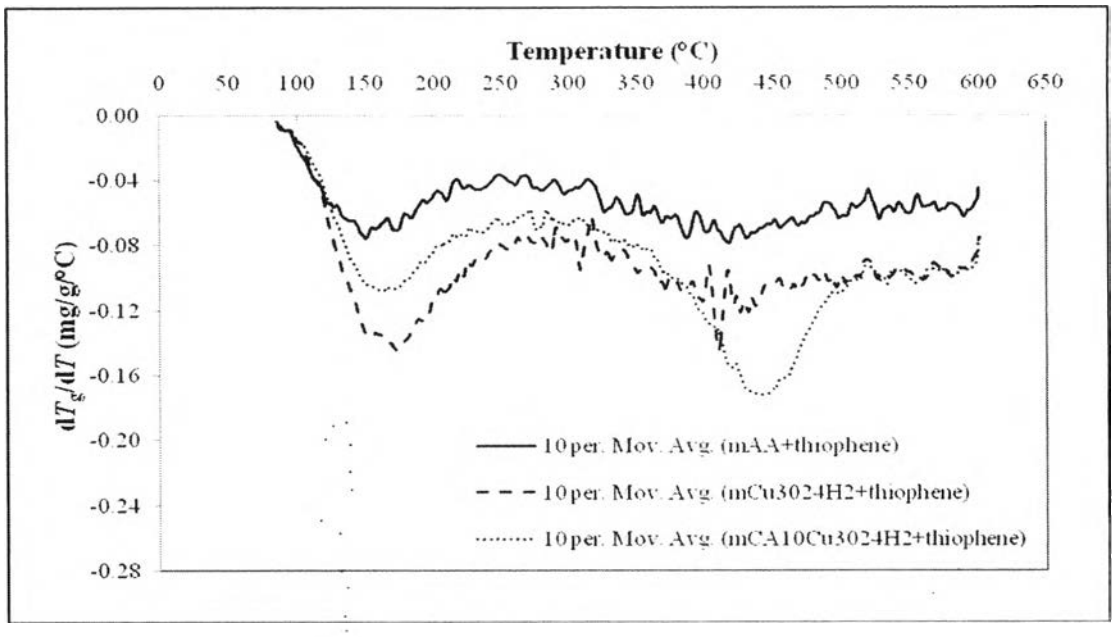

Figure 4.13 Desorption profiles of pure thiophene solution adsorbed on m-Al_2O_3, reduced 30% Cu/m-Al_2O_3 and reduced 30% Cu/m-Al_2O_3 modified with CA (Cu/CA=10).

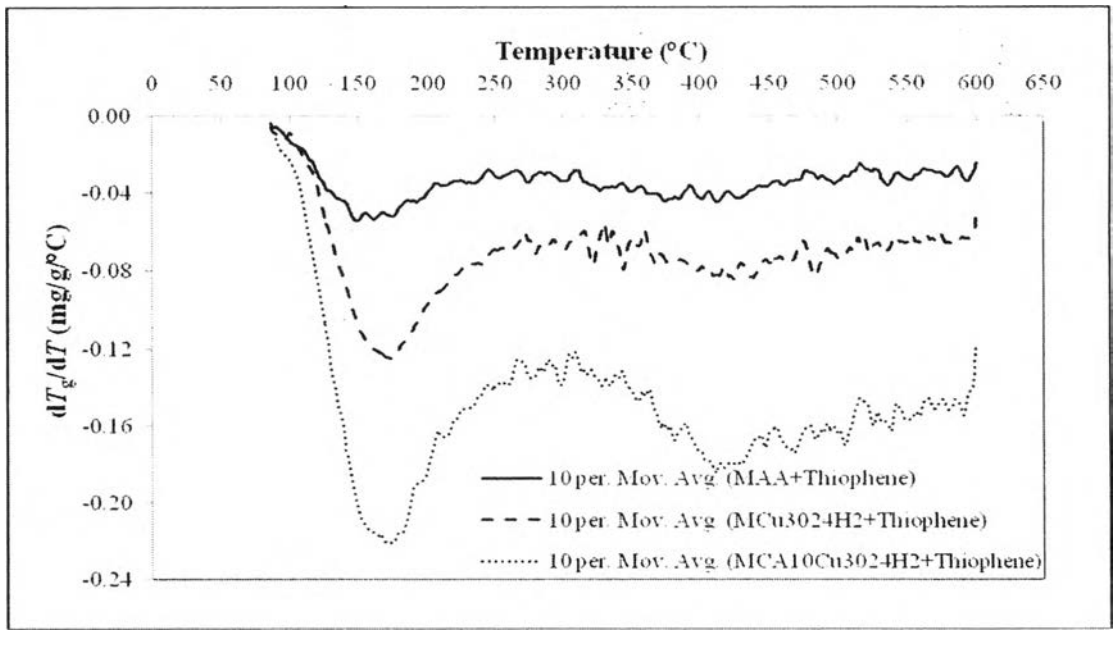

Figure 4.14 Desorption profiles of pure thiophene solution adsorbed on M-Al_2O_3, reduced 30% Cu/M-Al_2O_3 and reduced 30% Cu/M-Al_2O_3 modified with CA (Cu/CA=10).

From Figure 4.13 and Figure 4.14, they illustrate that the desorption temperature of thiophene adsorbed on both aluminas is approximately 160 °C, the desorption temperature of thiophene adsorbed on both reduced aluminas is approximately 175 °C which is identical with the desorption temperature of thiophene adsorbed on both reduced aluminas modified with CA (Cu/CA=10). The desorption temperature of thiophene on impregnated aluminas is higher than those on non-impregnated aluminas. It is observed that the impregnated adsorbents are better for adsorption due to the adsorbate–adsorbent interactions are higher. Thus, the impregnated aluminas is better to be used as a selective reomoval of sulfur compouds adsorbent.

It is in agreement with the XPS results which shown that the reduction step enhance the metal dispersion whether they were modified with CA or not. The main effect to metal dispersion is H_2 treatment (reduction step).

4.6.4 The Effect of Aromatics on Adsorptive Desulfurization

The selectively removal of sulfur compounds is an important parameter which is determined if the adsorbents are good to be used in desulfurization. The adsorption of aromatic compounds was studied in order to compare them with the adsorption of sulfur compounds. The better the adsorption, the higher the desorption temperature (harder to desorb). Therefore, the desorption profiles of toluene (aromatic compounds) and thiophene (sulfur compounds) adsorbed on both reduced aluminas modified with CA (Cu/CA=10) were studied.

Figure 4.15 and Figure 4.16 show the desorption profiles of pure toluene and pure thiophene solutions adsorbed on reduced 30% Cu/m-Al_2O_3 modified with CA (Cu/CA=10) and on reduced 30% Cu/M-Al_2O_3 modified with CA (Cu/CA=10), respectively.

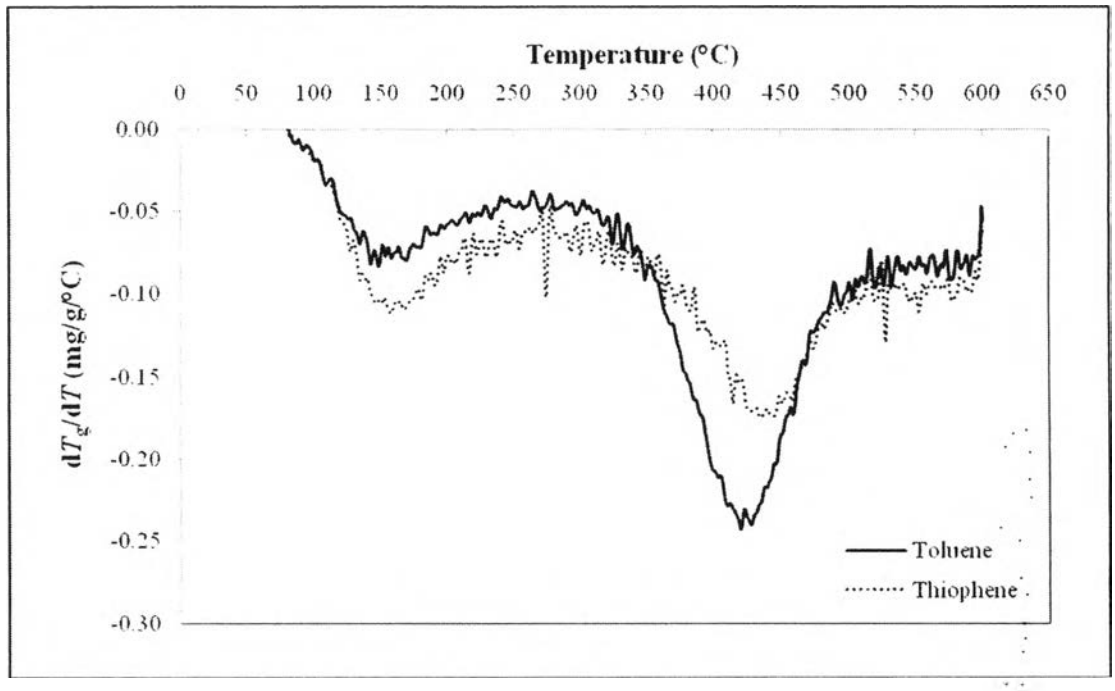

Figure 4.15 Desorption profiles of pure toluene and pure thiophene solutions adsorbed on reduced 30% Cu/m-Al_2O_3 modified with CA (Cu/CA=10).

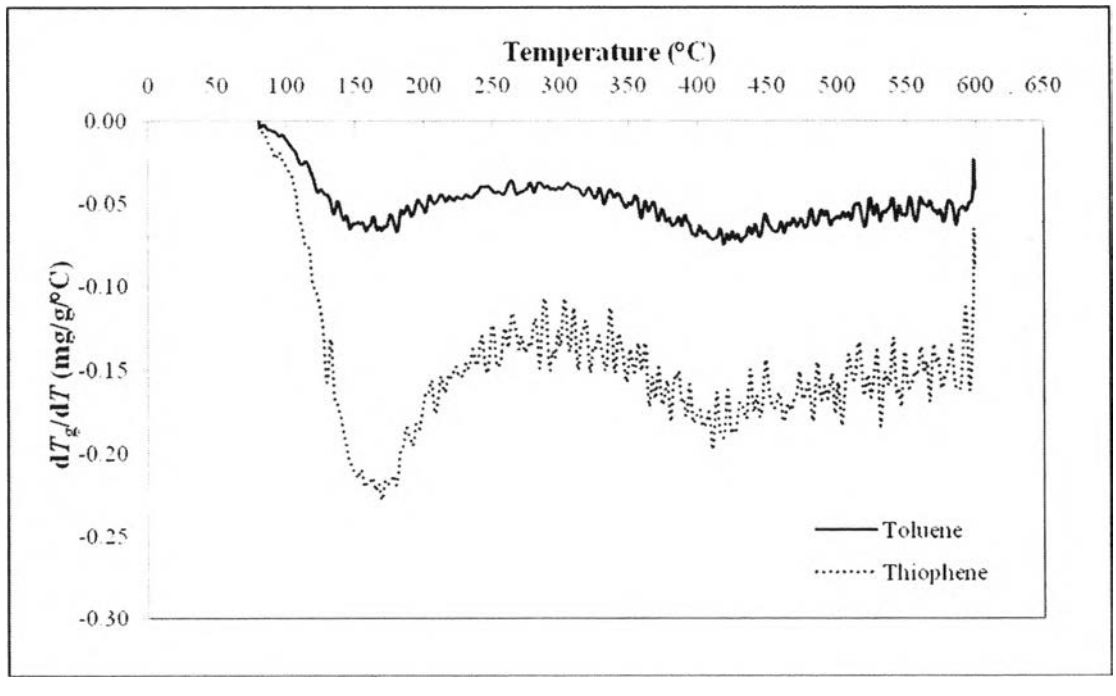

Figure 4.16 Desorption profiles of pure toluene and pure thiophene solutions adsorbed on reduced 30% Cu/M-Al_2O_3 modified with CA (Cu/CA=10).

From Figure 4.15 and Figure 4.16 show that the desorption temperature of toluene adsorbed on both adsorbents is approximately 150 °C whereas the desorption temperature of thiophene adsorbed on both adsorbents is approximately 160 °C. The desorption temperature of thiophene is higher than those of toluene about 10 °C even the molecular weight of thiophene (84.14 g/mol) is lower than toluene (92.14 g/mol). The molecular weight of adsorbate is not a major parameter. It is a specific interaction which is claimed as a π-complextion adsorption. Thus, there is a specific interaction between thiophene and the adsorbents. It implies that these adsorbents selectively remove thiophene (sulfur compound) over toluene (aromatic compound).

4.7 Inverse Gas Chromatography (IGC) Experiments

After column was stabilized under helium overnight, the non-polar (*n*-alkanes) and polar (toluene and thiophene) probe molecules were introduced to contact with the stationary phase (π-complexation adsorbents) in the column at working temperature by infinite dilution injection. For each measurement, at least two repeated injections were taken, obtaining reproducible results. The retention times were determined at the peak maxima. In the case of infinite dilution a symmetrical (Gaussian) peak is observed representing a linear (Henry's region) isotherm (Thielmann and Baumgarten, 2000). A typical gas chromatogram obtained for surface properties study at 225 °C on m-Al_2O_3 is shown in Figure 4.17. This figure illustrates the difference in retention time, when *n*-alkane probes (*n*-C_5, *n*-C_6, *n*-C_7, *n*-C_8, *n*-C_9 and *n*-C_{10}) and polar probes (toluene and thiophene) are injected consecutively within the column. The obtained peaks are symmetrical and retention times are reproducible. Similar chromatograms were obtained for the other materials. The summary of IGC data (an average of retention time, min) are shown in Appendix C.

Then, the specific retention volume was calculated by Equation (1) and the adsorption parameters (ΔH_{ads} and ΔG_{ads}) and thermodynamic parameters (γ_s^d and γ_s^s) were calculated by Equation (4) through Equation (12) aforementioned in chapter 3.

4.7.1 Influence of Injection Volume on the Measurements

The IGC experiments were performed at 250 °C with varying different amount of injection volume from 0.5–5.0 µL. Octane was chosen to be studied in this experiments. The carrier gas was helium at an adjusted flowrate of 2 nL/h. Figure 4.18 shows the specific retention volume as a function of injection volume for *n*-octane at 250 °C on non-impregnated mesoporous alumina (m-Al_2O_3), reduced 30% Cu/m-Al_2O_3 and reduced 30% Cu/m-Al_2O_3 modified with dispersing agent (CA), Cu/CA molar ratio of 5.

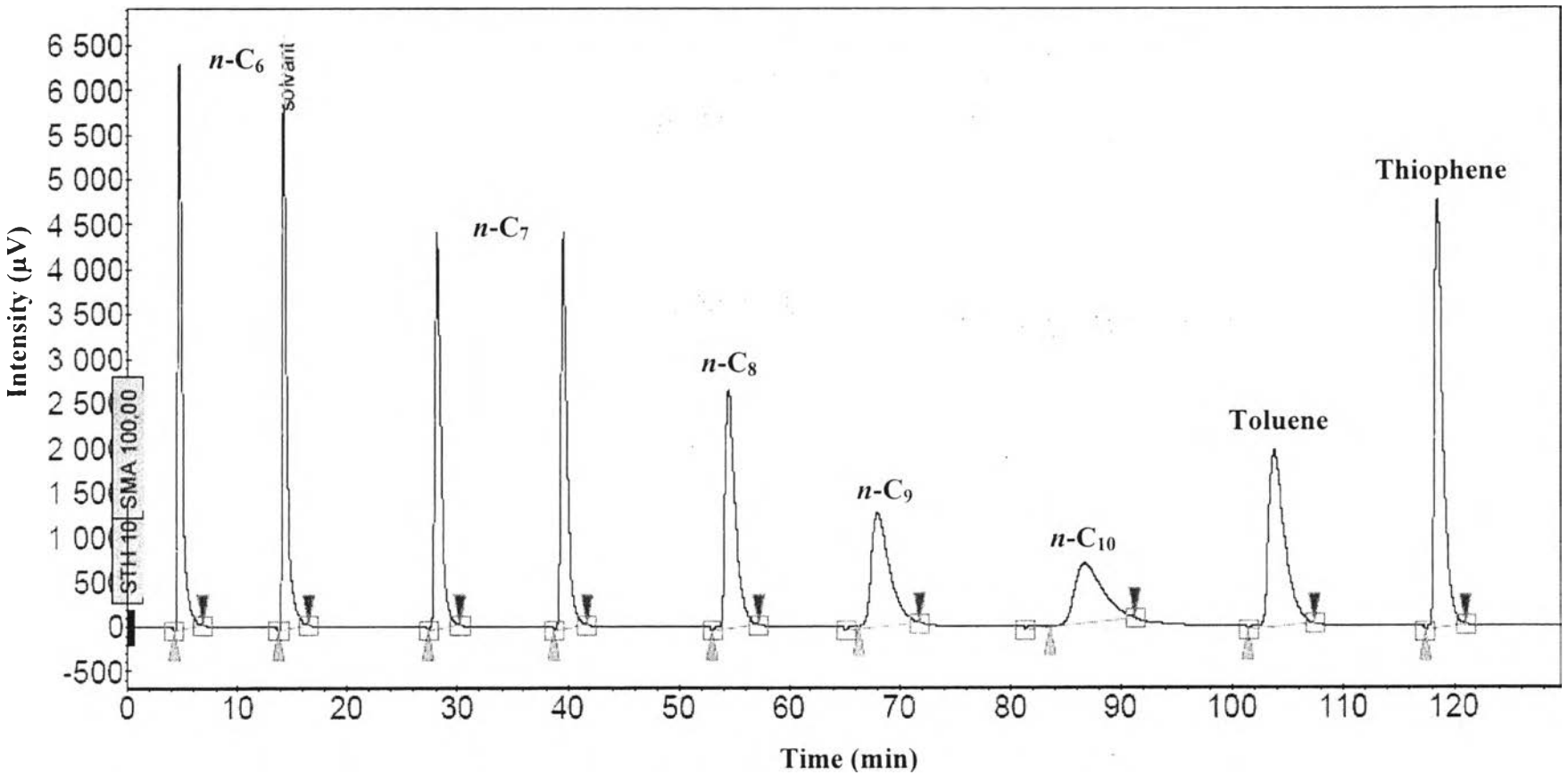

Figure 4.17 Typical gas chromatogram showing output signal following the consecutive injection of *n*-alkane probes (*n*-C_6–*n*-C_{10}) and polar probes (toluene and thiophene) at the same acquisition on m-Al_2O_3 obtained at 225 °C.

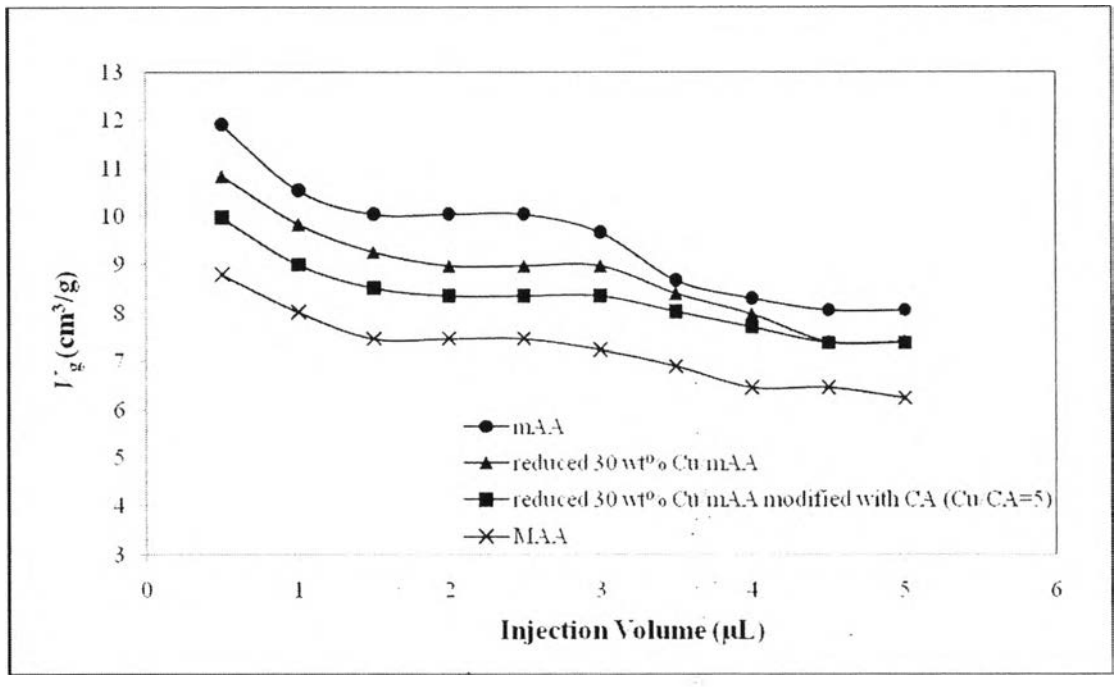

Figure 4.18 specific retention volume as a function of injection volume for *n*-octane at 250 °C on m-Al_2O_3 (●), reduced 30% Cu/m-Al_2O_3 (▲), reduced 30% Cu/m-Al_2O_3 modified with CA (Cu/CA = 5) (■) and M-Al_2O_3 (×).

It is observed that all the adsorbents show the same trend with three regions where in the first region, V_g decreases with increasing injection volumes, in the second region, V_g remains almost constant and in the third region, V_g increases with the injected volume. As a general trend, there are three region with aforementioned V_g and injection volume relationship, has been reported for polymers as stationary phases (Díaz, 2004a). This is unlikely to occur in this case, due to the high specific surface area of alumina as compared to polymers, and hence multilayer condensation does not take place. The first region of the curve in Figure 4.18 may correspond to a nonequilibrium situation. The third region of the curve in Figure 4.18 is attributed to the deviation of the Henry's region with non-infinite dilution injection, and therefore the adsorption for all the hydrocarbons and all the polar probes (toluene and thiophene) studied are based on data in the intermediate region.

It was found that the dependence of the adsorption on the injection volume for all the adsorbents studied is neglected for the range of injection volume

of 2.0–3.0 μL. According to Figure 4.18, an injection volume of 2.0 μL was chosen to carry out the study.

4.7.2 Enthalpy of Adsorption

Enthalpies of adsorption (ΔH_{ads}) can be obtained from the slope of a plot of $\ln V_g$ against $1/T$, based on Equation (3). The graph plotted $\ln V_g$ against $1/T$ for *n*-alkanes is shown in Figure 4.19, Figure 4.20 and Figure 4.21 for m-Al_2O_3, reduced 30% Cu/m-Al_2O_3 and M-Al_2O_3, respectively, and for polar probes (toluene and thiophene) is shown in Figure 4.22, Figure 4.23 and Figure 4.24 for m-Al_2O_3, reduced 30% Cu/m-Al_2O_3 and M-Al_2O_3, respectively.

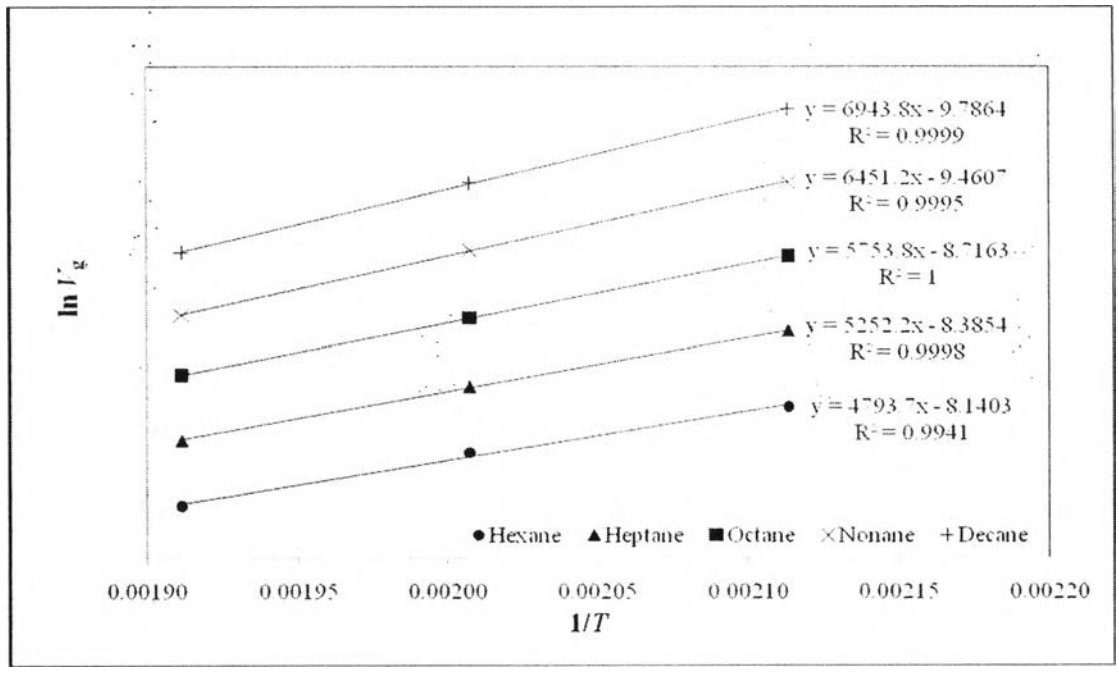

Figure 4.19 Determination of adsorption enthalpies of non-polar probes (*n*-alkanes) on m-Al_2O_3 at the temperature range between 200–250 °C: hexane (●), heptane (▲), octane (■), nonane (×) and decane (+).

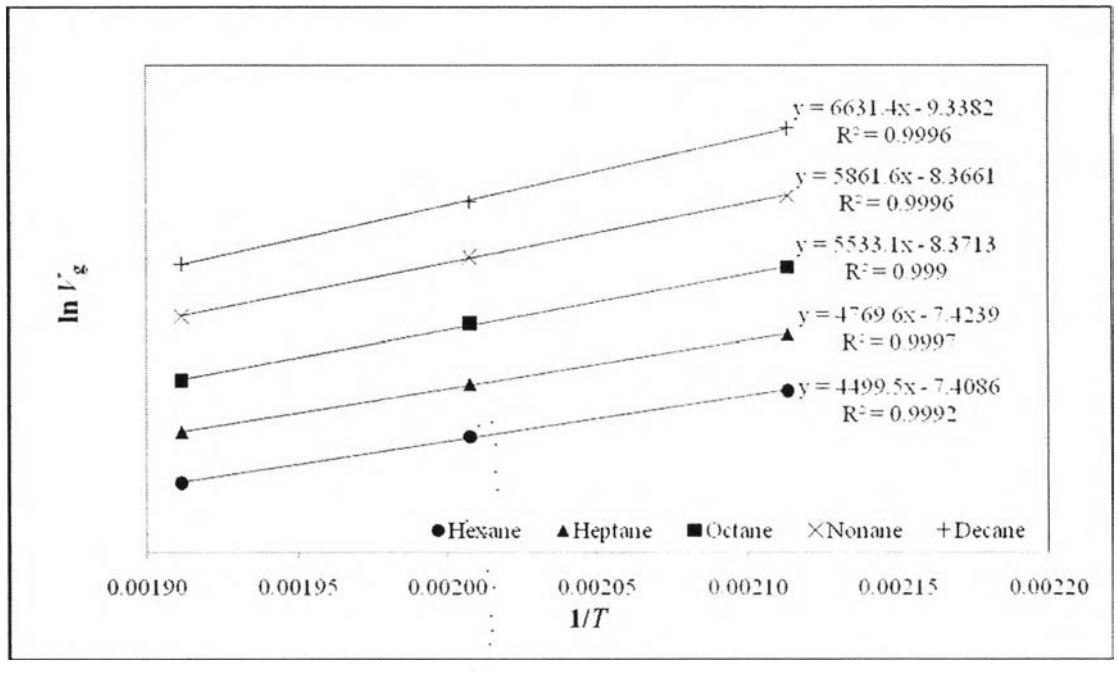

Figure 4.20 Determination of adsorption enthalpies of non-polar probes (*n*-alkanes) on reduced 30% Cu/m-Al_2O_3 at the temperature range between 200–250 °C: hexane (●), heptane (▲), octane (■), nonane (×) and decane (+).

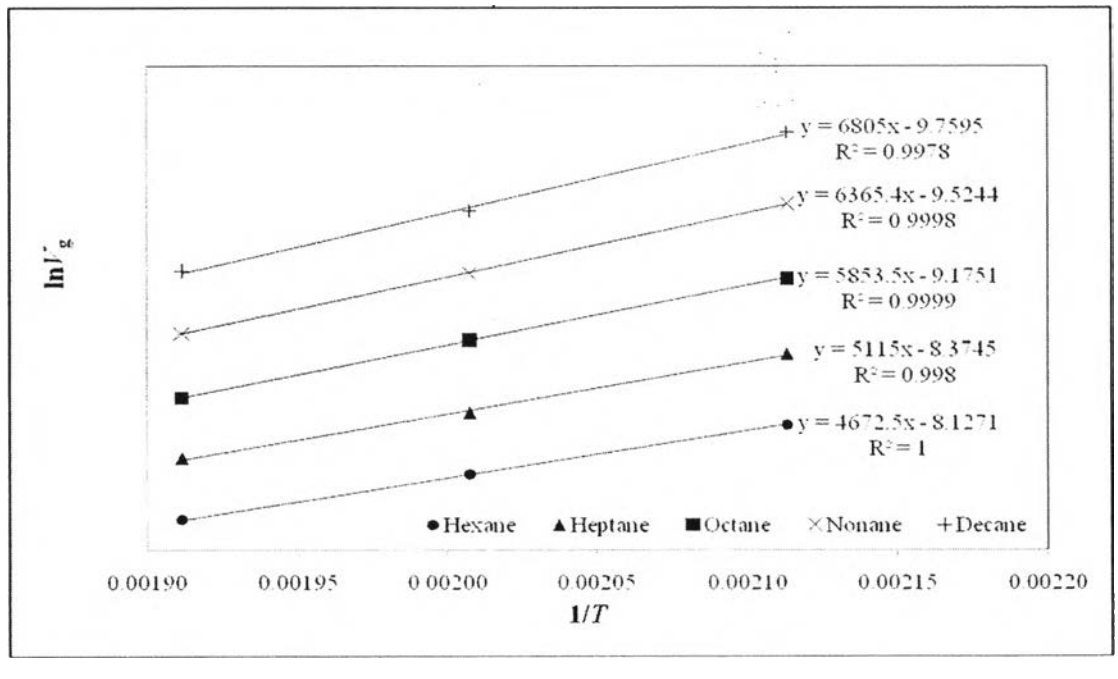

Figure 4.21 Determination of adsorption enthalpies of non-polar probes (*n*-alkanes) on M-Al_2O_3 at the temperature range between 200–250 °C: hexane (●), heptane (▲), octane (■), nonane (×) and decane (+).

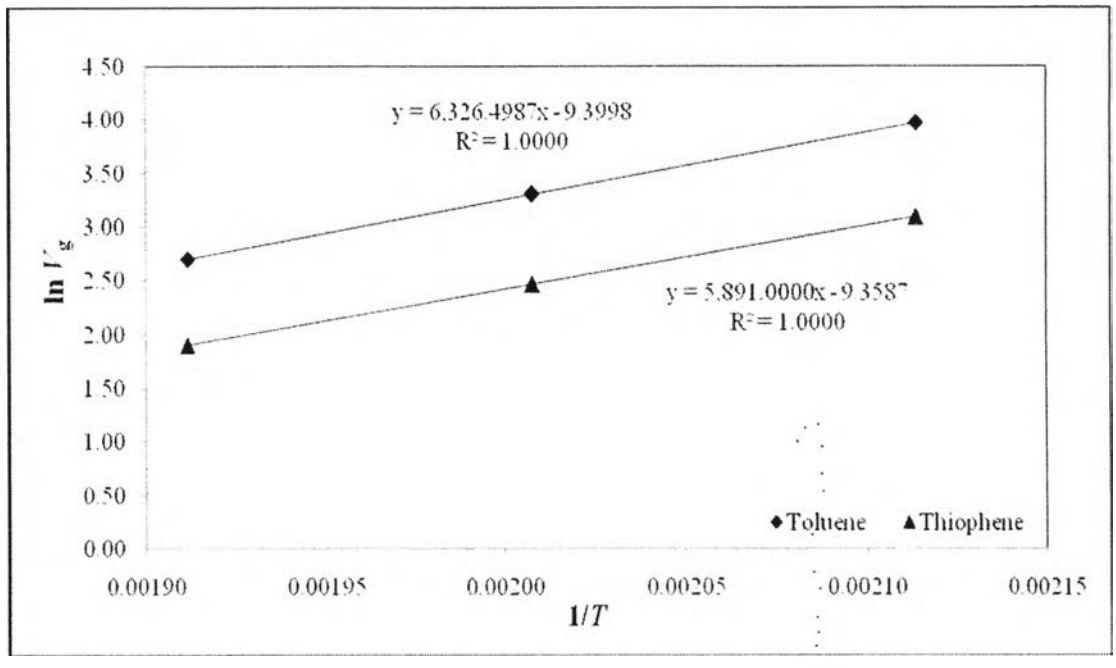

Figure 4.22 Determination of adsorption enthalpies of polar probes (toluene and thiophene) on m-Al_2O_3 at the temperature range between 200–250 °C: toluene (♦) and thiophene (▲).

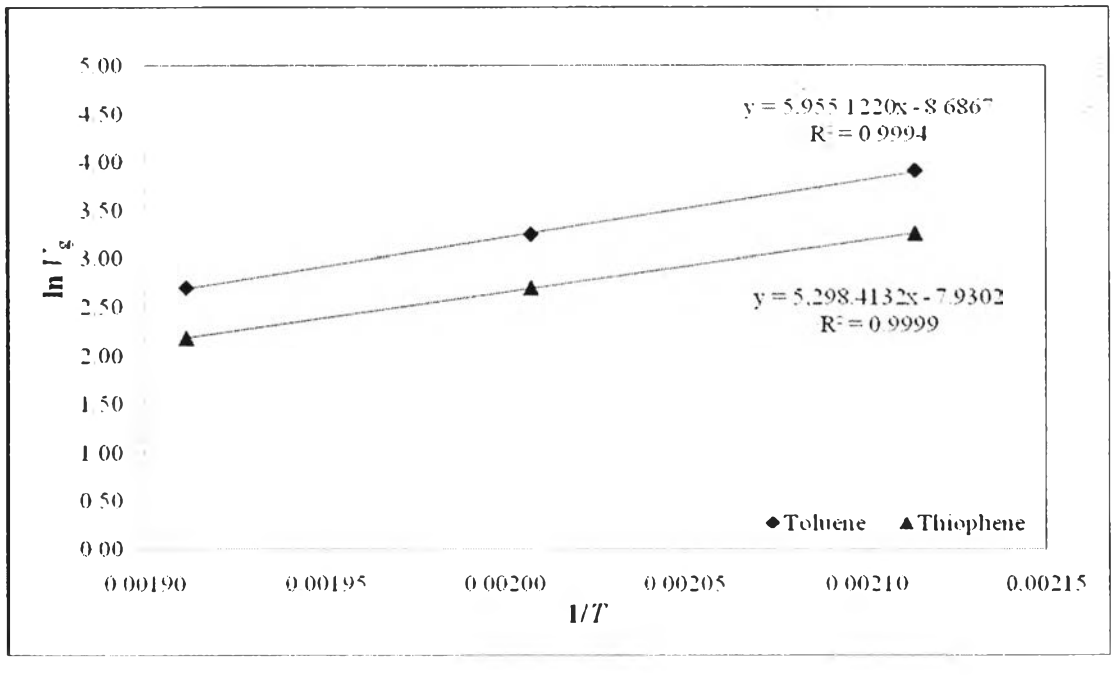

Figure 4.23 Determination of adsorption enthalpies of polar probes (toluene and thiophene) on reduced 30% Cu/m-Al_2O_3 at the temperature range between 200–250 °C: toluene (♦) and thiophene (▲).

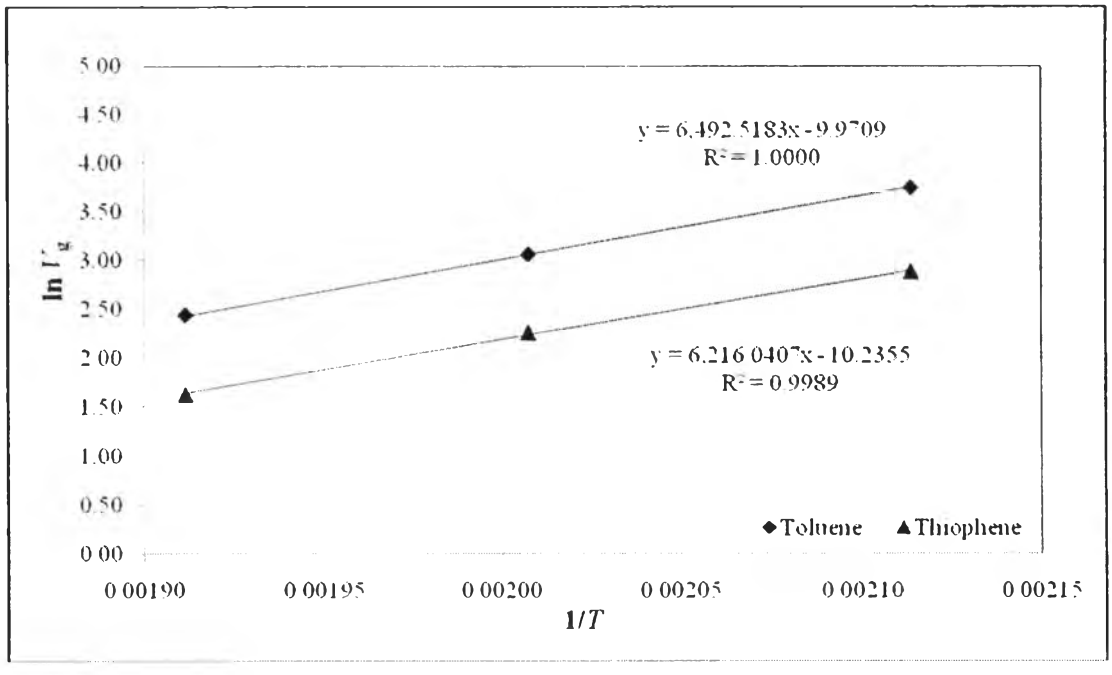

Figure 4.24 Determination of adsorption enthalpies of polar probes (toluene and thiophene) on M-Al_2O_3 at the temperature range between 200–250 °C: toluene (♦) and thiophene (▲).

From Figure 4.19 through Figure 4.24, it is observed that all the adsorbents studied in this experiments show their linear relation between the $\ln V_g$ and $1/T$ of all the non-polar and polar probe molecules, where their linear regression coefficient, R^2, are approximate to one. Thus, it is proved that this method is well fit with the theory which it exhibits such a good linear relation.

Adsorption enthalpies (ΔH_{ads}), were obtained from the slope of plots of $\ln V_g$ versus $1/T$ (from Figure 4.19 through Figure 4.24) then the Equation (3) was performed, shown in Figure 4.25, and results are summarized in Table 4.6.

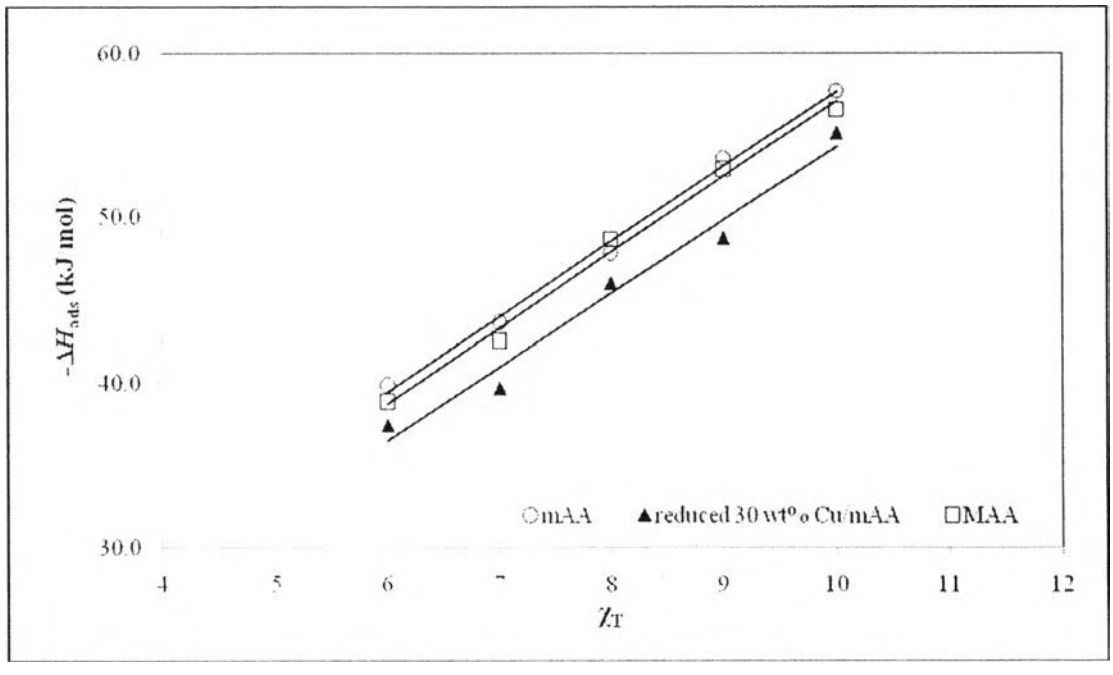

Figure 4.25 Adsorption enthalpies of *n*-alkanes on m-Al_2O_3 (○), reduced 30% Cu/m-Al_2O_3 (▲) and M-Al_2O_3 (□).

Table 4.6 Adsorption enthalpies ($-\Delta H_{ads}$) (kJ/mol) for the compounds studied over the different adsorbents

Probe Molecules		**Adsorbents**		
Chemical	χ_T	**m-Al_2O_3**	**Cu/m-Al_2O_3[a]**	**M-Al_2O_3**
Hexane	6	39.9	37.4	38.8
Heptane	7	43.7	39.7	42.5
Octane	8	47.8	46.0	48.7
Nonane	9	53.6	48.7	52.9
Decane	10	57.7	55.1	56.6
Toluene	6.26[b]	52.6	49.5	54.0
Thiophene	3.84[c]	49.0	44.1	51.7

[a] Reduced 30% Cu/m-Al_2O_3.

[b] Brendlé and Papirer, 1997b.

[c] See in Appendix B.

The adsorption enthalpies as a function of the adsorbate size, on m-Al_2O_3, reduced 30% Cu/m-Al_2O_3 and M-Al_2O_3 give a straight line, as shown in Figure 4.25. For all adsorbents the adsorption enthalpy of *n*-alkanes increases with the carbon number, due to the increasing boiling point of the *n*-alkanes and the stronger interaction between the solute and the adsorbent surface. It is in good agreement with the classical assumptions for adsorption processes: for the same family of compounds, the adsorption capacity increases with molecular weight as well as with its boiling temperature. High values of ΔH_{ads}, indicate a strong adsorbate–adsorbent interaction.

Similar results were found by Baumgarten *et al.* (1977) and Díaz *et al.* (2004a and 2004b) for the alumina when cyclohexane, benzene and *n*-alkanes adsorption were studied. Furthermore, Díaz *et al.* (2004b) found that the values of ΔH_{ads} were lower (superior in absolute value) to those of heats of liquefaction of these compounds (*n*-C_5–*n*-C_8). It implied that the enthalpies of adsorption measured were not only due to the heat of condensation of the compounds onto the surface, but also to physico-chemical interactions between solutes and adsorbents, i.e. the adsorbate–adsorbent interactions were preponderant for the initial experimental conditions and that the adsorbate–adsorbate interactions were negligible.

It is also observed that the adsorption enthalpies of *n*-alkanes on m-Al_2O_3 are quite identical compared with those on M-Al_2O_3. Besides, the adsorption enthalpies of *n*-alkanes on reduced 30% Cu/m-Al_2O_3 are lower than those on m-Al_2O_3 which is unexpected at first sight. It may correspond to the bad dispersion of the copper over the surface of alumina which is consistent with the SEM characterization results. Furthermore, this behavior is in a good agreement with the work published in the literature (Díaz *et al.*, 2004a; Skotak *et al.*, 2002) for the isomerization of alkanes (*n*-hexane, 2,2-dimethylbutane), in presence of hydrogen over a Pd/γ-Al_2O_3 catalyst. These authors also claim that Lewis acid sites are active for the adsorption of alkanes, the role of these acid sites being more important than the role of Pd in isomerization reactions. As described by the XRD characterization, after impregnation they form another chemicals which is in hydroxide form. It attributes to the surface modification which affect Lewis acid sites of the aluminas.

Therefore, at high copper loading impregnation will lead to lose the Lewis acid sites of aluminas, thus, the adsorption capacity of *n*-alkanes is reduced.

4.7.3 Free Energy of Adsorption

The free energies of adsorption for the five *n*-alkanes on m-Al_2O_3, reduced 30% Cu/m-Al_2O_3 and M-Al_2O_3 are shown in Figure 4.26 and the free energies of adsorption of different probes on m-Al_2O_3 at different temperatures are shown in Figure 4.27. Their results are given in Table 4.7, as calculated by performing Equation (4).

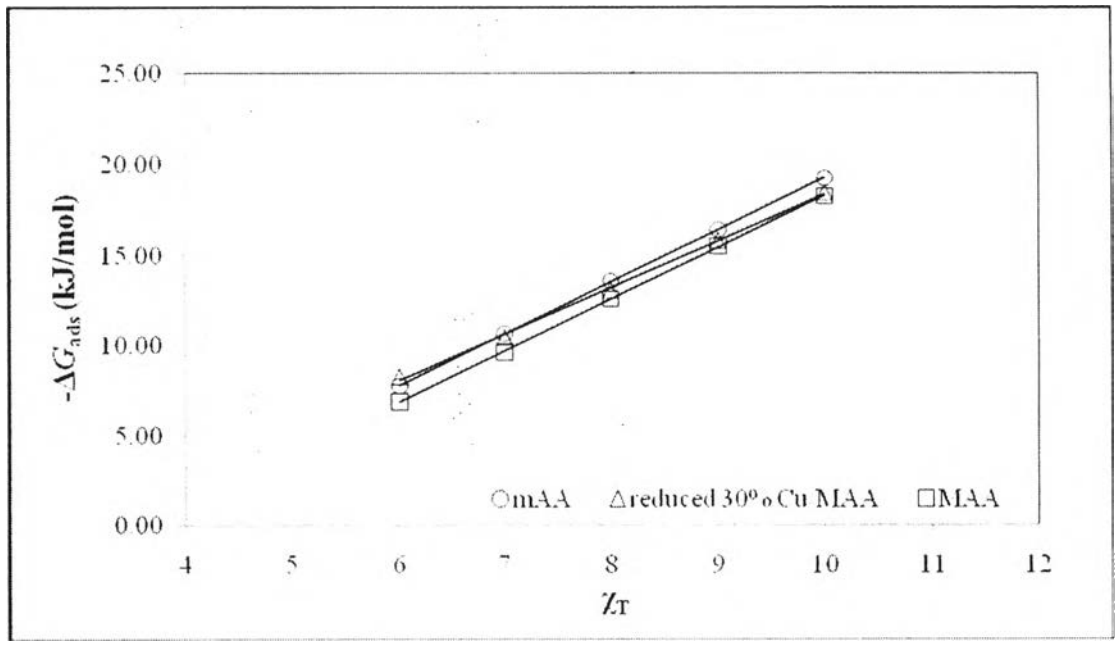

Figure 4.26 Adsorption free energies of *n*-alkanes on m-Al_2O_3 (○), reduced 30% Cu/m-Al_2O_3 (△) and M-Al_2O_3 (□) at 200 °C.

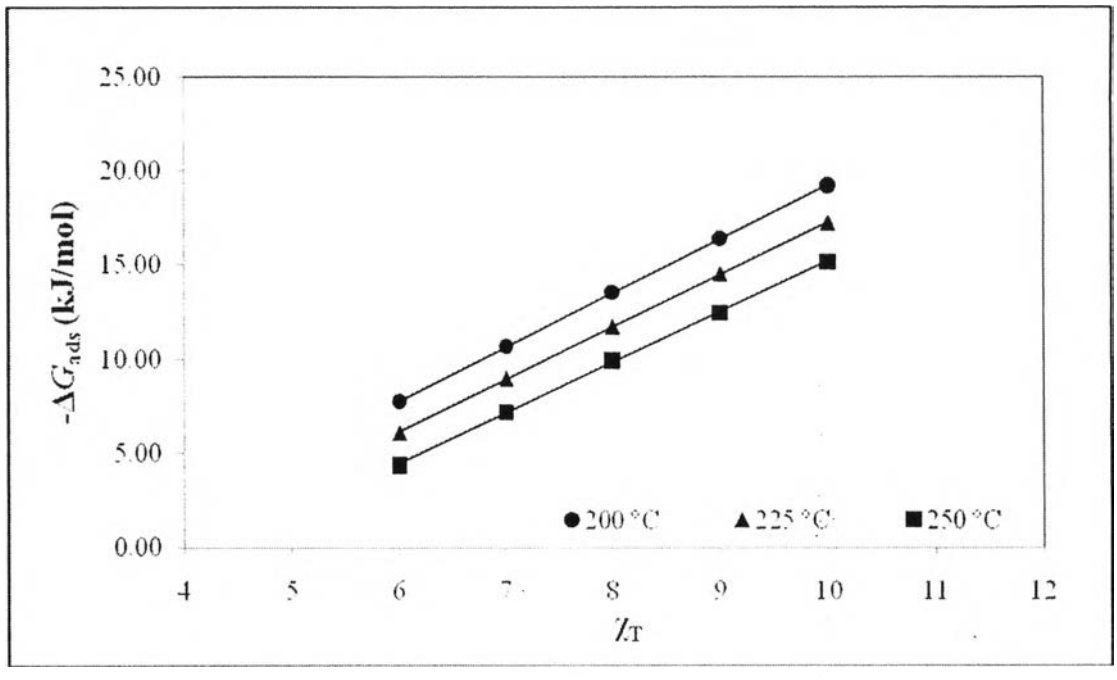

Figure 4.27 Free energy of different probe adsorptions on m-Al_2O_3 at different temperatures: 200 °C (●), 225 °C (▲) and 250 °C (■).

For a given adsorbate, the free energy of adsorption is the sum of energies of adsorption attributed to dispersive and specific interactions. The standard free energy of adsorption, ΔG_{ads}, takes into account the standard free energy of adsorption of polar solutes on solid surfaces, namely, the dispersive contribution, ΔG^{d}_{ads}, and the specific contribution, ΔG^{s}_{ads} which is corresponding to Equation (6) (Montes-Morán *et al.*, 2002). For *n*-alkanes, ΔG_{ads} is equal to ΔG^{d}_{ads} and changes with the number of carbon atoms in their molecules, the increment of adsorption energy corresponding to methylene group, ΔG_{CH_2}, and may be calculated from Equation (10). ΔG_{CH_2} is independent of the chosen reference state of adsorbed molecule. The slopes of linear functions given in Figure 4.26 and Figure 4.27 represent the increment in ΔG_{CH_2}. The values of ΔG_{CH_2} (kJ/mol) at different temperature are summarized in Table 4.8 and the procedures to get these values are described in Appendix C.

Data of ΔG_{ads} for the solute–adsorbent systems calculated from Equation (4), at different temperature, are given in Table 4.7. The free energy of adsorption for *n*-alkanes increases with the carbon number as shown in Figure 4.26. These results are in good agreement with the adsorption enthalpies that shown in Figure 4.25, the free energies of adsorption for all phases being very similar, and being a little higher for m-Al_2O_3 than for reduced 30% Cu/m-Al_2O_3 and M-Al_2O_3, respectively. The decrease in the adsorption free energy with increasing temperature, as shown in Figure 4.27, follows the van't Hoff equation.

Table 4.7 Standard free energy, $-\Delta G_{ads}$ (kJ/mol), for listed *n*-alkanes with m-Al_2O_3, reduced 30% Cu/m-Al_2O_3 and M-Al_2O_3

Adsorbents	Probe molecules		$-\Delta G_{ads}$ (kJ/mol), at		
	Chemical	χ_T	200 °C	225 °C	250 °C
m-Al_2O_3	Hexane	6	7.75	6.11	4.35
	Heptane	7	10.66	8.98	7.17
	Octane	8	13.55	11.74	9.93
	Nonane	9	16.39	14.52	12.45
	Decane	10	19.22	17.24	15.14
Reduced 30% Cu/m-Al_2O_3	Hexane	6	8.24	6.57	5.15
	Heptane	7	10.43	8.95	7.34
	Octane	8	13.03	11.42	9.54
	Nonane	9	15.80	14.14	12.31
	Decane	10	18.43	16.40	14.55
M-Al_2O_3	Hexane	6	6.87	5.00	3.50
	Heptane	7	9.63	7.73	6.16
	Octane	8	12.56	10.70	8.74
	Nonane	9	15.47	13.43	11.52
	Decane	10	18.24	16.00	14.21

4.7.4 Effect of Adsorption Temperature

From the study of free energy of adsorption as shown in Figure 4.26, Figure 4.27 and Table 4.7, the free energy of adsorption increases with decreasing of the adsorption temperature. It corresponds to higher in adsorbate–adsorbent interaction at lower adsorption temperature. It may imply that there is a good adsorption at lower temperature which is consistent with the thermodynamic phenomena, therefore the adsorption for all the hydrocarbons and all the polar probes (toluene and thiophene) studied by IGC experiments are carried out at the lowest adsorption temperature studied. The adsorption temperature of 200 °C was chosen to carry out the experiments.

4.7.5 Surface Free Energy

4.7.5.1 Dispersive Component

The interaction between *n*-alkanes and the stationary phase involves only dispersive forces. The dispersive components of the surface free energy, γ_s^d at different temperatures are summarized in Table 4.9. Figure 4.28 shows the dispersive component of the surface energy, γ_s^d, for m-Al_2O_3 and reduced 30% Cu/m-Al_2O_3, as a function of temperature. It is also noted that, as for the interaction parameters between *n*-alkanes adsorbent surface, the surface free energy of reduced 30% Cu/m-Al_2O_3 is lower than those of m-Al_2O_3 over the temperature range examined. This can be explained using the same arguments as in the case of the adsorption capacity and the enthalpy of adsorption. The dispersive component of the surface free energy, γ_s^d, also depends on the temperature. The dispersive interaction decreases as the temperature increases. This decrease is attributed to the entropic contribution to the surface free energy.

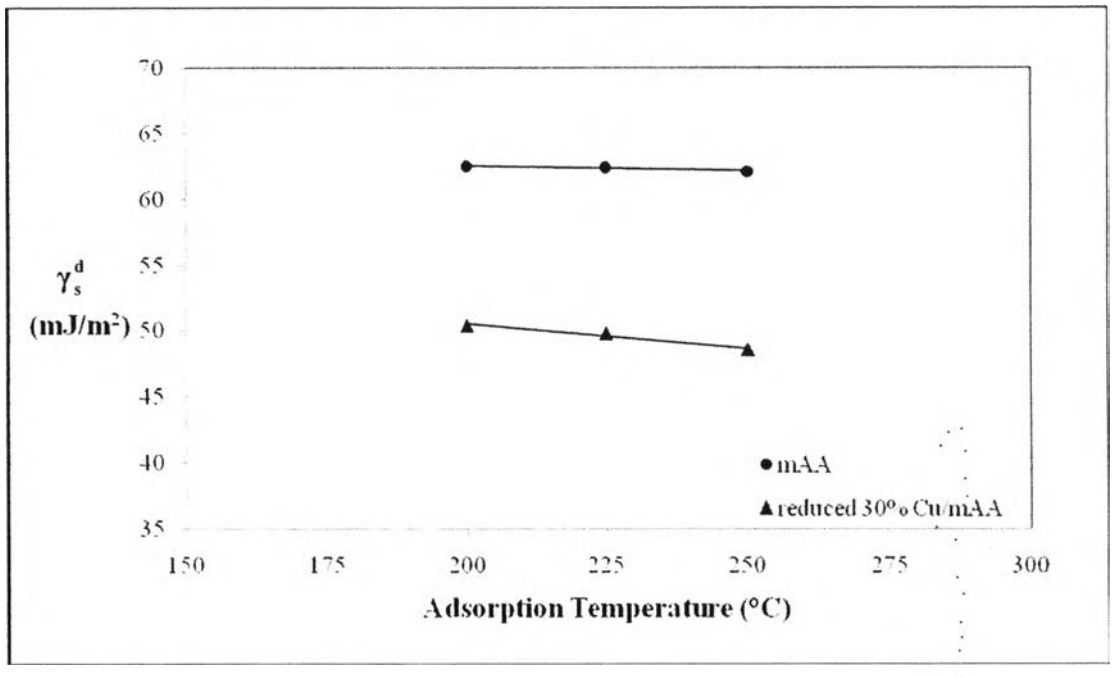

Figure 4.28 Dispersive component of the surface energy, γ_s^d, of m-Al_2O_3 (●) and reduced 30% Cu/m-Al_2O_3 (▲) as a function of temperature.

4.7.5.2 Specific Component

To complete the description of the surface properties, the specific forces have to be taken into account. The specific component (γ_s^s) of the surface free energy is closely related with the parameter of specific interaction of polar solutes (I^{sp}). They are generally caused by different interactions (either physical or electrical) between molecules. The specific interactions are the interactions other than London or dispersive interactions. This parameter involves the surface properties in terms of polar, ionic electrical, magnetic, metallic, and acid–base interactions and may be determined from the difference of free energy of adsorption, $\Delta(\Delta G)$, between a polar solute (toluene and thiophene) and the real or hypothetical corresponding *n*-alkanes (*n*-C_6–*n*-C_{10}).

The specific interaction, I^{sp}, determined for toluene and thiophene polar probe at different adsorption temperatures are tabulated in Table 4.10 and Table 4.11, respectively.

Table 4.8 ΔG_{CH_2} (kJ/mol) at different temperatures

Temperature (°C)	$-\Delta G_{CH_2}$, (kJ/mol)											
	mAA	MAA	mCu10 24H2	mCu20 24H2	mCu30 24H2	mCA05 Cu3024 H2	mNi10 24H2	mNi20 24H2	mNi30 24H2	MCu10 24H2	MCu20 24H2	MCu30 24H2
200	2.87	2.86	2.86	2.83	2.57	2.86	2.89	2.88	2.88	2.86	2.81	2.88
225	2.78	2.77	–	–	2.48	2.77	–	–	–	–	–	–
250	2.69	2.68	–	–	2.38	2.65	–	–	–	–	–	–

Table 4.9 Dispersive component of the surface free energy, γ_s^d (mJ/m^2) at different temperatures

Temperature (°C)	Dispersive component, γ_s^d (mJ/m^2)											
	mAA	MAA	mCu10 24H2	mCu20 24H2	mCu30 24H2	mCA05 Cu3024 H2	mNi10 24H2	mNi20 24H2	mNi30 24H2	MCu10 24H2	MCu20 24H2	MCu30 24H2
200	62.5	62.1	62.3	61.1	50.4	62.0	63.5	63.1	63.0	62.4	59.9	63.0
225	62.4	61.9	–	–	49.8	61.8	–	–	–	–	–	–
250	62.1	61.7	–	–	48.6	60.5	–	–	–	–	–	–

Table 4.10 Specific interaction, I^{sp} (mJ/m^2) at different temperatures (determined by toluene polar probe)

Temperature (°C)	Specific interaction, I^{sp}, (mJ/m^2) for toluene											
	mAA	MAA	mCu10 24H2	mCu20 24H2	mCu30 24H2	mCA05 Cu3024 H2	mNi10 24H2	mNi20 24H2	mNi30 24H2	MCu10 24H2	MCu20 24H2	MCu30 24H2
200	34.3	39.3	36.4	36.9	29.2	37.1	34.5	37.2	40.5	35.2	39.5	40.2
225	32.9	38.2	–	–	27.1	35.3	–	–	–	–	–	–
250	31.8	35.7	–	–	26.8	34.3	–	–	–	–	–	–

Table 4.11 Specific interaction, I^{sp} (mJ/m^2) at different temperatures (determined by thiophene polar probe)

Temperature (°C)	Specific interaction, I^{sp}, (mJ/m^2) for thiophene											
	mAA	MAA	mCu10 24H2	mCu20 24H2	mCu30 24H2	mCA05 Cu3024 H2	mNi10 24H2	mNi20 24H2	mNi30 24H2	MCu10 24H2	MCu20 24H2	MCu30 24H2
200	61.8	67.9	62.8	77.4	57.1	77.3	61.0	64.4	68.0	66.5	70.9	80.5
225	58.8	65.6	–	–	56.1	76.1	–	–	–	–	–	–
250	56.3	59.6	–	–	56.0	71.8	–	–	–	–	–	–

Figure 4.29 shows the specific interaction, I^{sp}, for m-Al_2O_3 and reduced 30% Cu/m-Al_2O_3 and reduced 30% Cu/m-Al_2O_3 modified with CA (Cu/CA=5), as a function of temperature. The specific interaction also depends on the temperature. It decreases as the temperature increases. This decrease is attributed to the entropic contribution to the surface free energy.

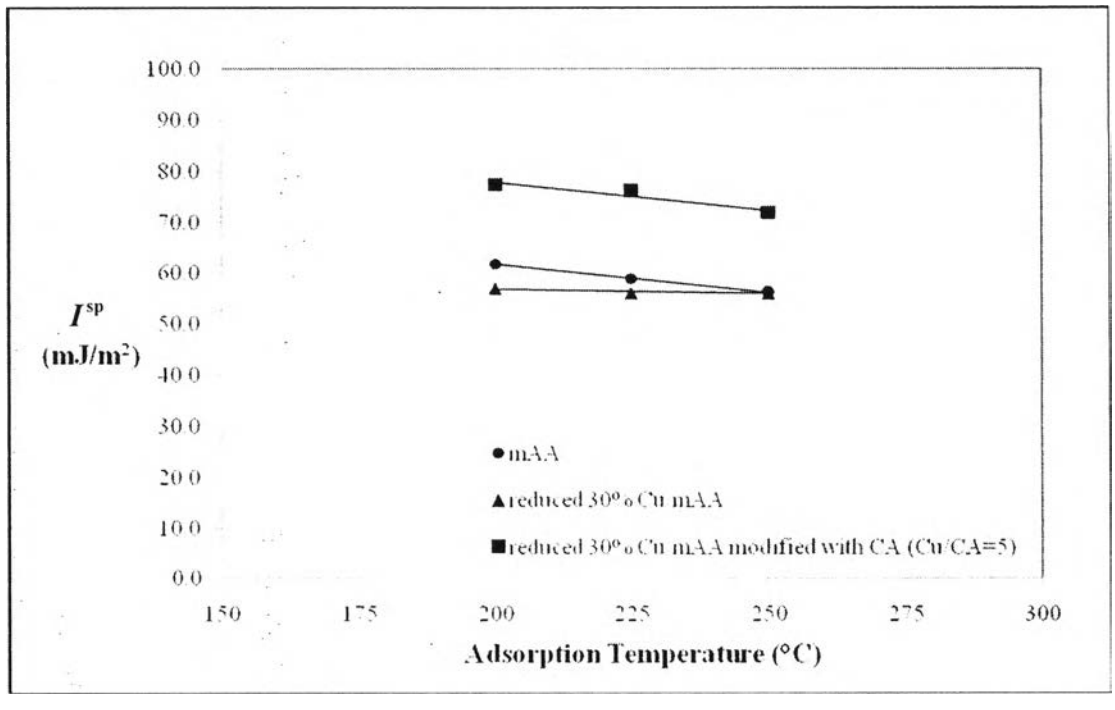

Figure 4.29 Specific interaction, I^{sp}, of m-Al_2O_3 (●), reduced 30% Cu/m-Al_2O_3 (▲) and reduced 30% Cu/m-Al_2O_3 modified with CA (Cu/CA=5) (■) determined by thiophene polar probe as a function of temperature.

Table 4.12 shows the ratio of specific interaction of thiophene over toluene obtained from the IGC experiments at 200 °C when toluene and thiophene were used as polar probe solutes.

Table 4.12 The specific interaction ratio of thiophene over toluene on various adsorbents examined by IGC experiments obtained at 200 °C when toluene and thiophene were used as polar probe solutes

Adsorbents	Specific Interaction Ratio
Support: Mesoporous Alumina	
m-Al_2O_3	1.80
Reduced 10% Cu/m-Al_2O_3	1.73
Reduced 20% Cu/m-Al_2O_3	2.10
Reduced 30% Cu/m-Al_2O_3	1.96
Reduced 30% Cu/m-Al_2O_3 modified with CA (Cu/CA=5)	2.09
10% Ni/m-Al_2O_3	1.77
20% Ni/m-Al_2O_3	1.73
30% Ni/m-Al_2O_3	1.68
Support: Macroporous Alumina	
M-Al_2O_3	1.73
Reduced 10% Cu/M-Al_2O_3	1.89
Reduced 20% Cu/M-Al_2O_3	1.79
Reduced 30% Cu/M-Al_2O_3	2.00

It is observed that the specific interaction of thiophene is higher than those of toluene with around 1.7–2.1 fold positive effect. It is indicated that these adsorbents are selectively adsorbing organosulfur molecules (thiophene) over aromatic ones (toluene). The best ratio that indicates the best selective adsorption capacity is around 2.9 which corresponds to reduced 30% Cu/m-Al_2O_3 modified with CA (Cu/CA=5) adsorbents. It is in a good agreement with the SEM, XPS and TPD characterization results which the H_2 treatment and dispersing agent modification give more positive effect on metal dispersion. Therefore, the modified adsorbents by H2 treatment and dispersing agent have a good sulfur adsorption result by means of IGC experiments.

4.7.6 Effect of Type of Adsorbent

Mesoporous and macroporous aluminas were studied in this work in order to examine the effect of type of these adsorbents on adsorptive desulfurization. It is studied by the IGC experiments with the determination of the specific interaction of both polar probe molecules (toluene and thiophene). The results are graphically shown in Figure 4.30 showing the specific interaction of thiophene (bold) and toluene (light) obtained from IGC characterization on different type of adsorbent.

After performing incipient wetness impregnation on these adsorbents, the effect of type of adsorbent is studied again by comparing the results of specific interaction of polar probe molecules on reduced 30% Cu/m-Al_2O_3 and reduced 30% Cu/M-Al_2O_3 shown in Figure 4.31.

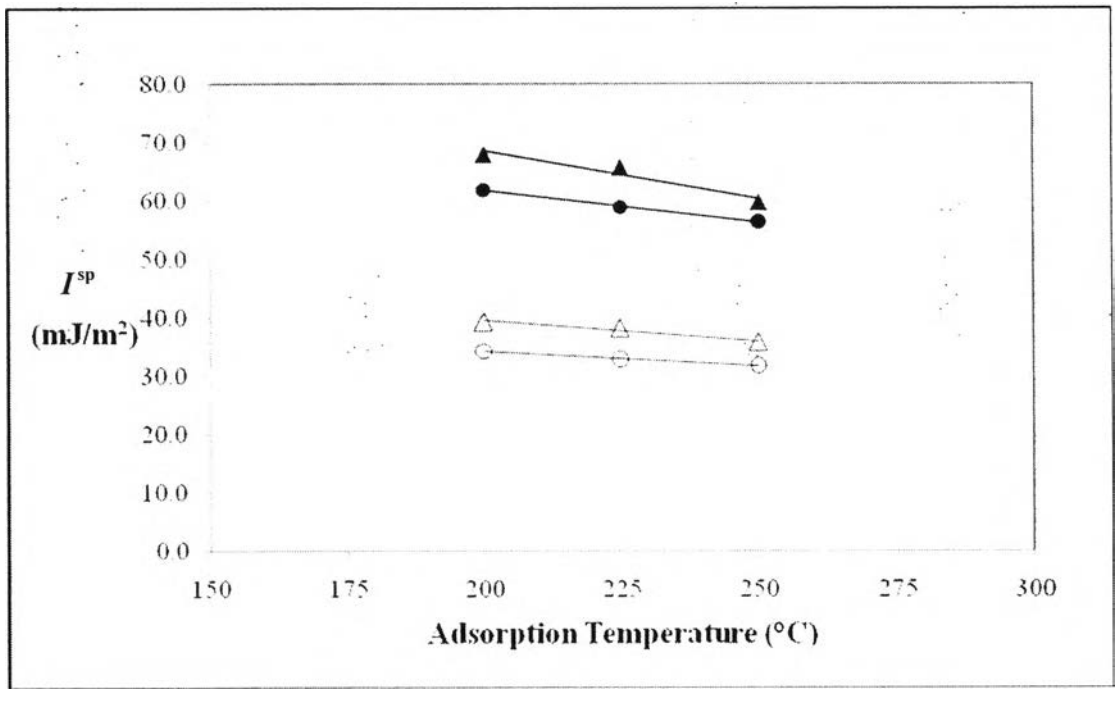

Figure 4.30 Specific interaction of toluene and thiophene on both aluminas as a function of temperature: I^{sp} of toluene on m-Al_2O_3 (○), I^{sp} of toluene on M-Al_2O_3 (Δ), I^{sp} of thiophene on m-Al_2O_3 (●) and I^{sp} of thiophene on M-Al_2O_3 (▲).

Figure 4.30 shows that the specific interaction of polar probe molecules on both unmodified aluminas is identical as there is a slight difference in the value obtained. It is hardly to indicate that the different type of adsorbent (in terms of pore size of alumina) is not affected to adsorptive desulfurization. Therefore, the study of impregnated aluminas is observed.

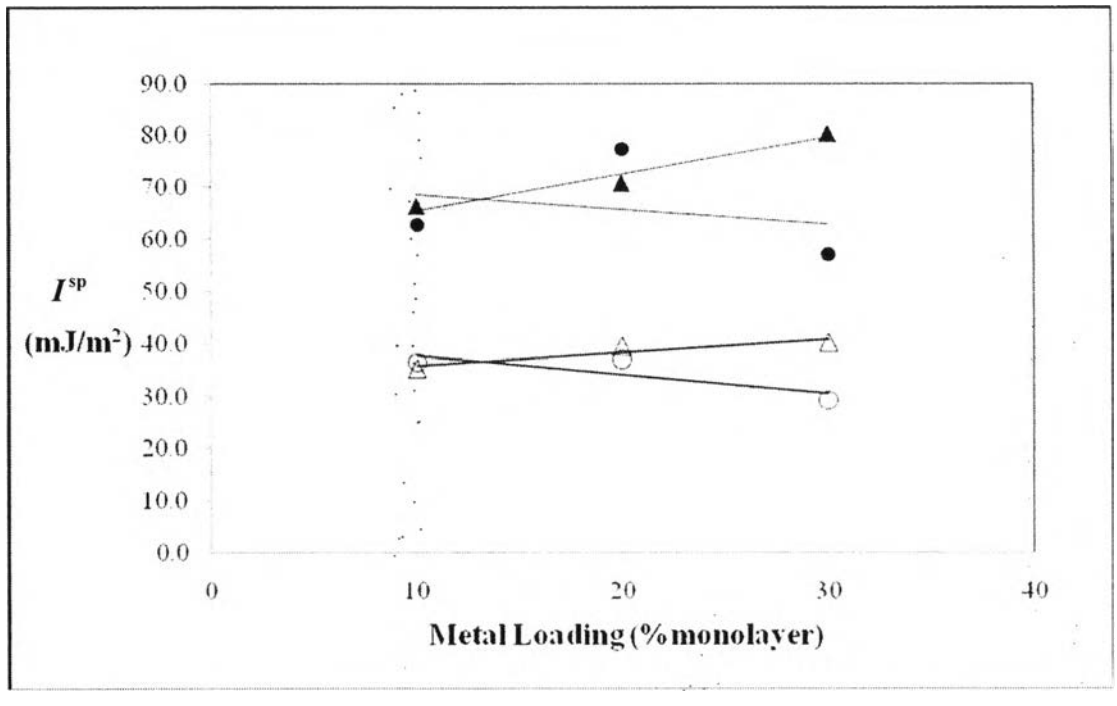

Figure 4.31 Specific interaction of toluene and thiophene on reduced Cu/m-Al_2O_3 and reduced Cu/M-Al_2O_3 as a function of metal loading: I^{sp} of toluene reduced Cu/m-Al_2O_3 (○), I^{sp} of toluene on reduced Cu/M-Al_2O_3 (Δ), I^{sp} of thiophene on reduced Cu/m-Al_2O_3 (●) and I^{sp} of thiophene on reduced Cu/M-Al_2O_3 (▲) obtained at 200 °C.

Figure 4.31 shows that the specific interaction of toluene and thiophene on reduced 30% Cu/m-Al_2O_3 decreases as the amount of metal loading increases, whereas the specific interaction of toluene and thiophene on reduced 30% Cu/M-Al_2O_3 increases with amount of metal loading. This behavior may be explained considering the relevance of the pore size of alumina. Hence, the impregnation is controlled by the diffusion of metal precursor into the pores,

therefore, to enter those macropores may easier, and the agglomeration of those metal in mesoporous alumina is easier than that in macroporous alumina. In case of m-Al_2O_3, high metal loading impregnation leads to worse of metal dispersion due to the metal cannot enter well in the pores. It is in good agreement with SEM characterization. Furthermore, the modification of these adsorbents by impregnation may affect the Lewis acid sites of alumina as described before. Therefore, the worse metal dispersion which lowers the π-complexation capacity constitutes to lower specific interaction between the polar probe molecules and adsorbents. For M-Al_2O_3, there is no limitation of diffusion due to the size of pores. Therefore, the capacity of π-complexation adsorption increases with the amount of metal loading. It is observed that macroporous alumina is better to be used as support for the adsorptive desulfurization adsorbents than mesoporous alumina.

4.7.7 Effect of Type of Metal Impregnation

In this work, Cu and Ni were used to impregnate on alumina to give their π-complexation adsorption ability in order to use these adsorbents to selectively remove organosulfur compounds.

The specific interaction of toluene and thiophene on different adsorbents modified by Cu and Ni impregnation at different metal loadings are shown in Figure 4.32 and Figure 4.33, respectively.

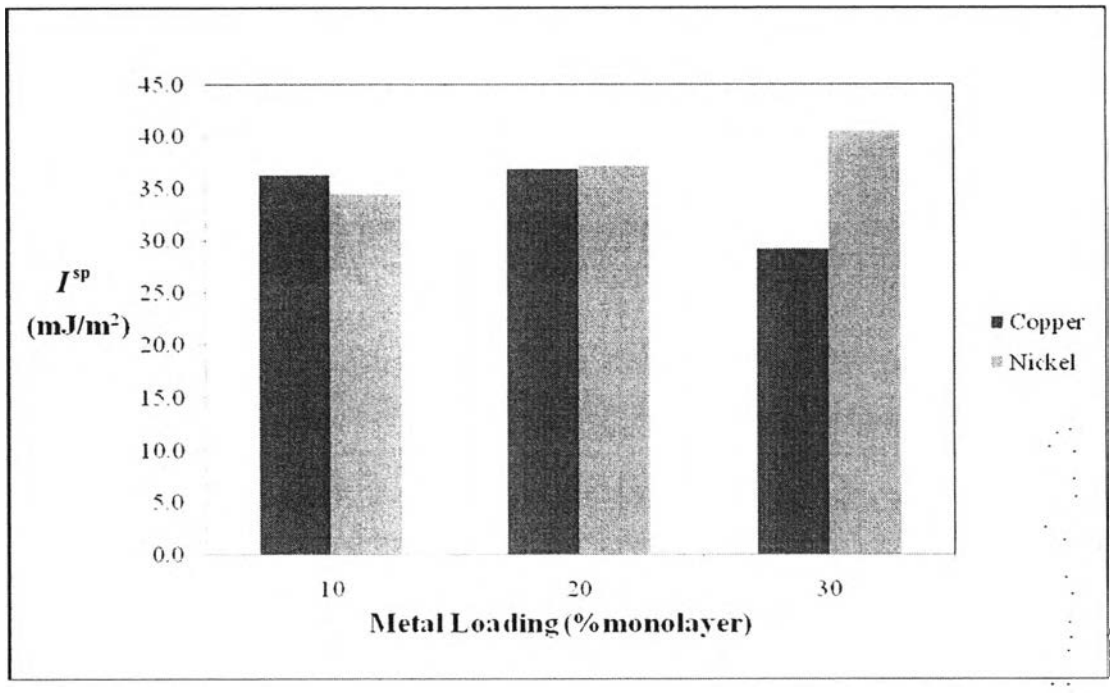

Figure 4.32 Specific interaction of toluene on reduced Cu/m-Al_2O_3 and Ni/m-Al_2O_3 as a function of metal loading obtained at 200 °C.

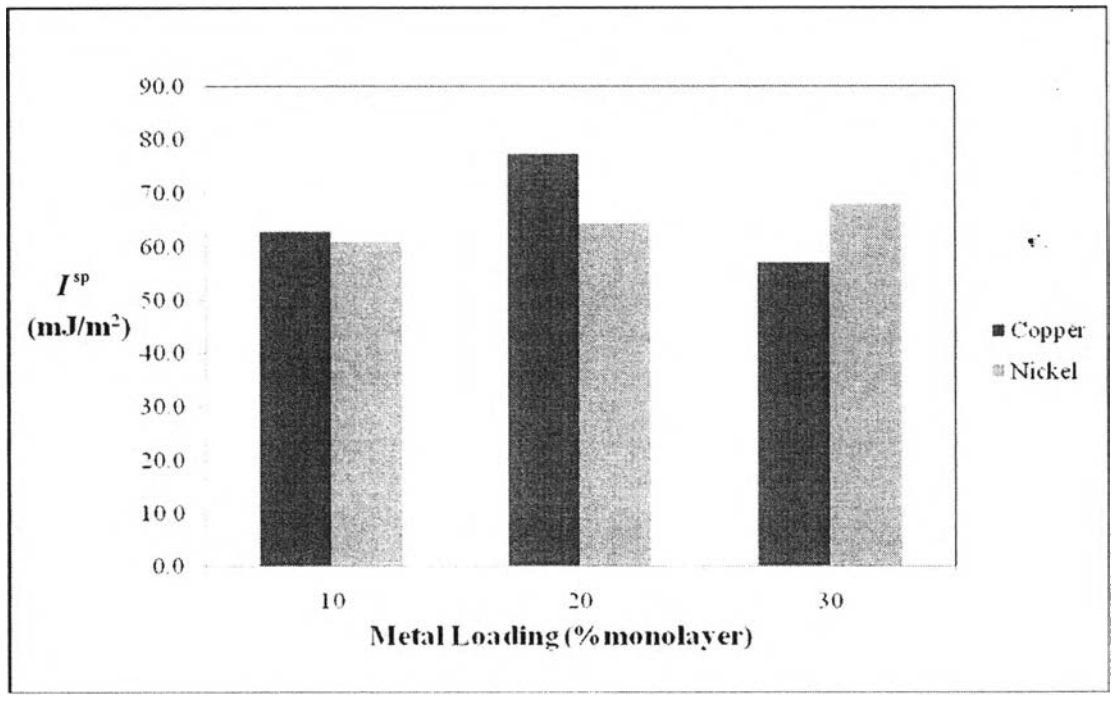

Figure 4.33 Specific interaction of thiophene on reduced Cu/m-Al_2O_3 and Ni/m-Al_2O_3 as a function of metal loading obtained at 200 °C.

Figure 4.32 and Figure 4.33 shows that the specific interaction of polar probe molecules on those adsorbents is quite the same. There are insignificant differences as the values obtained are slightly different. It cannot be clearly indicate that there is the effect of type of metal impregnation. Therefore, the effect of type of metal impregnation is insignificant in this experiment.

4.7.8 Effect of Amount of Metal Loading

The variation of amount of metal loading was done at 10, 20 and 30% of theoretical monolayer coverage. The specific interactions of polar probe molecules observed on those adsorbents are illustrated in Figure 4.31, Figure 4.32 and Figure 4.33. In case of nickel impregnation, it is shown that I^{sp} increases with the amount of metal loading which corresponds to the fact that there are more active sites to be bonded with the solutes. Thus, the I^{sp} is enhanced by this metal impregnation. But for the case of copper, the trend is inversed. This behavior can be explained by the same arguments that described in the effect of type of adsorbent part.

4.7.9 Effect of Dispersing Agent

There is a limitation of reduced 30% Cu/m-Al_2O_3 adsorbent in terms of adsorptive desulfurization (determined by specific interaction) as the adsorption capacity is the lowest among adsorbents studied. To study the effect of dispersing agent, reduced 30% Cu/m-Al_2O_3 modified with CA (Cu/CA=5) was observed. The results are shown in Figure 4.34.

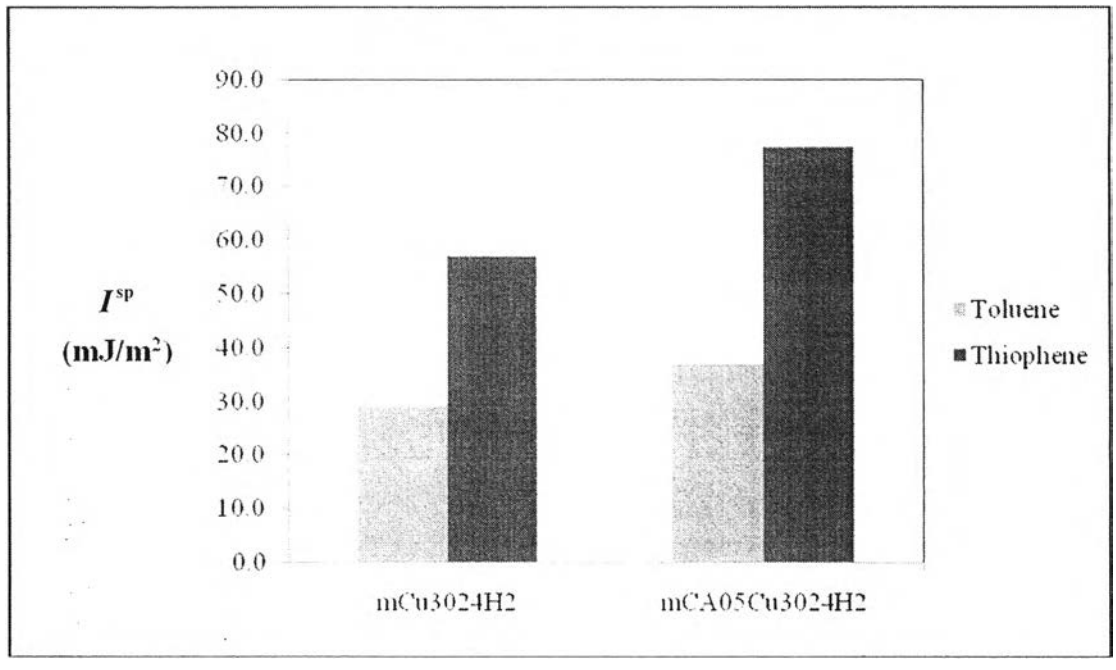

Figure 4.34 Specific interaction of toluene and thiophene on reduced 30% Cu/m-Al_2O_3 and reduced 30% Cu/m-Al_2O_3 modified with CA (Cu/CA=5) obtained at 200 °C.

Figure 4.34 shows the I^{sp} of toluene and thiophene on reduced 30% Cu/m-Al_2O_3 and reduced 30% Cu/m-Al_2O_3 modified with CA (Cu/CA=5). It is shown that there is an extinct results obtained from the IGC experiments. Comparing the I^{sp} of toluene together and also of the thiophene shows that the adsorption capacity is improved significantly. Therefore, dispersing agent gives a positive effect on the adsorptive desulfurization which exhanced around 1.2 times compared to those of unmodified adsorbents. It was in a good agreement with SEM characterization, XPS results and TPD by TGA-MS experiments.